I. Remarks

Claims 1-24, 31-59, and 67-74 are pending.

In order to comply with the restriction requirement, claims 25-30 and 60-66 directed to the non-elected invention have been deleted. Applicants retain the right to pursue the subject matter of these claims in future continuation or divisional applications.

Claims 3 and 38 are withdrawn as being directed to a non-elected species. Applicants respectfully request that the examiner consider these additional species claims upon the allowance of a generic claim to which these species claims depend from or otherwise require all the limitations of, as provided by 37 CFR 1.141.

Claims 1, 24, 35, 36 and 74 have been amended to more clearly define the invention. Support for the amendment that an oncogene operably linked to a promoter induces an oncogenic phenotype can be found throughout the specification, for example in Examples 1 and 2. No issues of new matter should arise and entry of the amendment is respectfully requested.

II. Specification

The disclosure is objected to because the description of Figure 13 does not refer to part (D). Applicants have amended the description to refer to part (D) of the figure. In view thereof, the objection to the specification is moot.

III. Enablement

Claims 1, 2, 4-24, 31-37, 39-59, and 67-74 are rejected under 35 USC 112, first paragraph, for allegedly lacking enablement for 1) a transgenic fish whose genome

comprises any oncogene operably linked to any promoter wherein the oncogene is not expressed and does not cause an oncogenic phenotype or 2) a method of using the fish as claimed. Applicants respectfully traverse this rejection.

The claims as amended are directed to transgenic fish whose genome has stably integrated therein an oncogene operably linked to a promoter, wherein the oncogene induces an oncogenic phenotype. Applicants have shown at least two working examples of the claimed transgenic fish. In example 1, Applicants have shown transgenic fish expressing a cMYC oncogene operably linked to a Rag2 promoter, wherein the oncogene induced T-cell acute lymphoblastic leukemia. In example 2, Applicants have shown transgenic fish expressing a BCL2 oncogene operably linked to a Rag2 promoter, wherein the oncogene induced an anti-apoptotic phenotype. In examples 3-5, Applicants have shown prophetic examples of transgenic fish models of astrocytomas, rhabdomyosarcomas, and acute myeloid leukemia. Despite the multiple examples provided, the examiner asserts that the specification does not provide the guidance necessary to make a transgenic fish expressing any oncogene other than cMYC operably linked to a Rag2 promoter, due to the unpredictability of making transgenic animals.

Contrary to what the examiner has asserted, Applicants submit that the person of ordinary skill who understood and appreciated the teachings of the specification would recognize that heterologous promoters in fish could express an oncogene, in levels sufficient to result in an oncogenic phenotype. It is known that the organization of the human genome as well as the genetic pathways controlling signal transduction and development are highly conserved in zebrafish, and that these properties have established that the zebrafish is an excellent model system for studies of vertebrate developmental

mechanisms and human diseases, including cancers. See, for example, Langenau (2003) *Science* 299: 877-890; Postlethwait (2000) *Genome Res.* 10: 1890-1902; Liu (2002) *PNAS USA* 99: 6136-6141; Bennett (2001) *Blood* 98, 643-651.

Applicants' position is amply supported by post-filing art that demonstrates, at the time of Applicants' invention, it would not require undue experimentation to develop transgenic fish models of oncogenes operably linked to promoters, wherein an oncogenic phenotype is expressed, other than the specifically disclosed cMYC linked to Rag2 embodiment. For example, Sabaawy and coworkers, who do not include any of the inventors on the present application, developed transgenic zebrafish expressing TEL-AML1 as a model of precursor B cell acute lymphoblastic leukemia (abstract attached as Appendix A). Inventor Langenau and coworkers developed a zebrafish system of RAS-induced rhabdomyosarcoma (abstract of paper submission attached as Appendix B). Inventor Look and coworkers developed a transgenic zebrafish expressing BRAF mutations under the control of the melanocyte mitfa promoter, wherein the transgenic fish developed invasive melanomas (abstract attached as Appendix C). In another example, Inventor Look was also involved in developing a zebrafish transgenic model of pancreatic endocrine carcinoma, by generating fish that expressed a human MYCN transgene under the control of a zebrafish myod promoter (paper attached as Appendix D).

Further, as examples of other promoters that have been shown to drive expression of a heterologous gene in the zebrafish model, Example 5 of the instant application discloses that numerous zebrafish promoters have been identified as capable of driving strong expression of GFP, including the PU.1, MPO, or C/EBPα promoters (see also

references attached as Appendices E and F).

It is submitted that these post-filing references establish that transgenic fish models have been successfully developed for T-cell oncogenes, B-cell oncogenes, tissue-specific promoters, and lymphoid-specific promoters, and that this was possible as of the filing date without undue experimentation by the ordinarily skilled person.

In view of the demonstrated ability to develop numerous transgenic fish models of oncogenes operably linked to promoters, wherein an oncogenic phenotype is expressed, other than the specifically disclosed cMYC linked to Rag2 embodiment, Applicants respectfully submit that it would not require undue experimentation to carry out the invention as claimed.

With respect to the method claims drawn to screening for drugs that modulate, either positively or negatively, oncogene-mediated neoplastic or hyperplastic transformation, the examiner asserts that a use for positive modulation is not readily apparent. Applicants respectfully submit that a use for a drug that increases oncogene-mediated neoplastic or hyperplastic transformation would be readily apparent to the person of ordinary skill. For example, a patient with genetic mutation that is identified as suppressing oncogene-mediated neoplastic or hyperplastic transformation could be treated with a drug that increases oncogene-mediated neoplastic or hyperplastic transformation to test whether the drug reverses the effects of the genetic mutation. As another example, a patient treated with a first drug or agent that is identified as suppressing oncogene-mediated neoplastic or hyperplastic transformation could be treated with a second drug that increases oncogene-mediated neoplastic or hyperplastic transformation to test whether the second drug reverses the effects of the first drug.

The examiner further asserts that the claims encompass treatment of a fish to determine whether an agent, for example, decreases expression of leukemic markers or number of tumors and that this cannot be done with an untreated sibling control as a means of comparison. Applicants respectfully traverse this part of the rejection. The claims as amended require that the oncogene induces an oncogene-mediated neoplastic or hyperplastic transformation, and a determination is made as to whether the test drug or agent modulates the oncogene-mediated neoplastic or hyperplastic transformation. Applicants respectfully submit that the person of ordinary skill would not need a second untreated fish as a means of comparison, because the person would not need to look beyond the treated fish itself to determine whether the drug modulates the oncogenic phenotype of the fish. By looking at the treated fish before and after treatment with a drug, a determination can be made as to whether the drug modulates the oncogene-induced phenotype. The person of ordinary skill would understand that the fish prior to treatment is the means of comparison to the fish after the treatment. Therefore, no comparison fish is necessary to carry out the method of the invention.

In view of the foregoing, Applicants respectfully submit that the claims as amended are fully enabled by the application. Withdrawal of this rejection is respectfully requested.

IV. Written Description

Claims 18 and 53 are rejected under 35 USC 112 as allegedly failing to comply with the written description requirement. Applicants respectfully traverse this rejection.

Applicants have provided in the specification an adequate description of

"substantially similar" oncogenes. See, for example, the definition at the paragraph bridging pages 21 and 22, where "substantially similar" is defined as sufficiently similar to a reference nucleotide that a nucleotide sequence will hybridize to the reference nucleotide under moderately stringent conditions. As noted in the specification, moderately stringent conditions are well known in the art. The specification further requires that a "substantially similar" oncogene encode a protein having cell neoplastic transformation ability.

Applicants respectfully submit that the specification provides adequate written description of "substantially similar" oncogenes. In view thereof, withdrawal of this rejection is respectfully requested.

V. Indefiniteness

Claims 18 and 53 are rejected under 35 USC 112, second paragraph as allegedly being indefinite.

As discussed above, Applicants have provided a definition of "substantially similar" in the specification such that one of skill in the art would understand the metes and bounds of the claims. In view thereof, withdrawal of this rejection is respectfully requested.

VI. Conclusion

Applicants respectfully request that the outstanding rejections be withdrawn. An early and favorable consideration and allowance of the pending claims is respectfully requested.

Respectfully submitted,

Belinda Lew

Belinda Lew, Ph.D.
Registration No. 53,212
Agent for Applicants

Date: March 22, 2007

Wilmer Cutler Pickering Hale and Dorr LLP
1875 Pennsylvania Avenue, NW
Washington, DC 20006
202-663-6029 (telephone)
202-663-6363 (facsimile)

APPENDIX A

Published online before print October 2, 2006, 10.1073/pnas.0603349103
PNAS | **October 10, 2006** | vol. 103 | no. 41 | **15166-15171**

◄ Previous Article | Table of Contents | Next Article ►

BIOLOGICAL SCIENCES / MEDICAL SCIENCES

TEL-AML1 transgenic zebrafish model of precursor B cell acute lymphoblastic leukemia

Hatem E. Sabaawy[†,‡], Mizuki Azuma[†], Lisa J. Embree[†], Huai-Jen Tsai[§], Matthew F. Starost[¶], and Dennis D. Hickstein[†]

[†]Experimental Transplantation and Immunology Branch, Center for Cancer Research, National Cancer Institute, Bethesda, MD 20892; [§]Institute of Molecular and Cellular Biology, National Taiwan University, Taipei 10617, Taiwan; and [¶]Division of Veterinary Resources, Office of Research Services, National Institutes of Health, Bethesda, MD 20892

Edited by Ernest Beutler, The Scripps Research Institute, La Jolla, CA, and approved August 16, 2006 (received for review April 24, 2006)

This Article
- Figures Only
- Full Text
- Full Text (PDF)
- Supporting Information
- Alert me when this article is cited
- Alert me if a correction is posted
- Citation Map

Services
- Similar articles in this journal
- Similar articles in PubMed
- Alert me to new issues of the journal
- Add to My File Cabinet
- Download to citation manager
- Request Copyright Permission

Google Scholar
- Articles by Sabaawy, H. E.
- Articles by Hickstein, D. D.

PubMed
- PubMed Citation
- Articles by Sabaawy, H. E.
- Articles by Hickstein, D. D.
- Pubmed/NCBI databases
  - Gene
  - GEO Profiles
  - Nucleotide
  - Protein
  - UniGene

Acute lymphoblastic leukemia (ALL) is a clonal disease that evolves through the accrual of genetic rearrangements and/or mutations within the dominant clone. The *TEL-AML1* (*ETV6-RUNX1*) fusion in precursor-B (pre-B) ALL is the most common genetic rearrangement in childhood cancer; however, the cellular origin and the molecular pathogenesis of *TEL-AML1*-induced leukemia have not been identified. To study the origin of *TEL-AML1*-induced ALL, we generated transgenic zebrafish expressing *TEL-AML1* either ubiquitously or in lymphoid progenitors. *TEL-AML1* expression in all lineages, but not lymphoid-restricted expression, led to progenitor cell expansion that

evolved into oligoclonal B-lineage ALL in 3% of the transgenic zebrafish. This leukemia was transplantable to conditioned wild-type recipients. We demonstrate that *TEL-AML1* induces a B cell differentiation arrest, and that leukemia development is associated with loss of *TEL* expression and elevated *Bcl2/Bax* ratio. The *TEL-AML1* transgenic zebrafish models human pre-B ALL, identifies the molecular pathways associated with leukemia development, and serves as the foundation for subsequent genetic screens to identify modifiers and leukemia therapeutic targets.

stem cell | translocation | childhood cancer | genetics

Author contributions: H.E.S., L.J.E., and D.D.H. designed research; H.E.S. and M.F.S. performed research; H.E.S., H.-J.T., and M.F.S. contributed new reagents/analytic tools; H.E.S., M.A., L.J.E., and D.D.H. analyzed data; and H.E.S. and D.D.H. wrote the paper.

The authors declare no conflict of interest.

This paper was submitted directly (Track II) to the PNAS office.

‡To whom correspondence should be addressed. E-mail: sabaawyh@mail.nih.gov

APPENDIX B

Identification of an Evolutionarily Conserved RAS Signature and the Cancer Stem Cell in Embryonal Rhabdomyosarcoma

David M. Langenau1, Matthew D. Keefe1, Narie Y. Storer1, Jeffrey R. Guyon2, Jeffery L. Kutok3, Xiuning Le1, Wolfram Goessling1, Donna Neuberg4, Louis M. Kunkel2, and Leonard I. Zon1

1 Stem Cell Program and Division of Hematology/Oncology, Children's Hospital Boston and Dana-Farber Cancer Institute, Boston, MA 02115
2 Program in Genomics and Howard Hughes Medical Institute at Children's Hospital Boston, Boston, MA 02115
3 Department of Pathology, Brigham and Women's Hospital, Boston, MA 02115
4 Dana-Farber Cancer Institute, Boston, MA 02115

Running Title: Zebrafish RAS-induced rhabdomyosarcoma
Key words for indexing: zebrafish, rhabdomyosarcoma, RAS, P53, and transgenic

Abstract
Embryonal rhabdomyosarcoma (ERMS) is a devastating cancer with specific features of muscle differentiation that can result from mutational activation of RAS family members; however to date, RAS pathway activation has not been reported in a majority of ERMS patients. Here, we have created a zebrafish model of RAS-induced ERMS, in which animals develop externally-visible tumors by 10 days of life. Microarray analysis and cross-species comparisons identified two conserved gene signatures found in both zebrafish and human ERMS, one associated with stage-specific and tissue-restricted gene expression in rhabdomyosarcoma and a second comprising a novel RAS-induced gene signature. Remarkably, our analysis uncovered that RAS pathway activation is exceedingly common in human RMS. We also created a new transgenic co-injection methodology to fluorescently-label distinct sub-populations of tumor cells based on muscle differentiation status. In conjunction with FACS sorting, cell transplantation, and limiting dilution analysis, we were able to identify the cancer stem cell in zebrafish ERMS. When coupled with gene expression studies of this cell population, we propose that the activated satellite cell is the target for transformation in embryonal rhabdomyosarcoma.

APPENDIX C

1: Curr Biol. 2005 Feb 8;15(3):249-54.

BRAF mutations are sufficient to promote nevi formation and cooperate with p53 in the genesis of melanoma.

Patton EE, Widlund HR, Kutok JL, Kopani KR, Amatruda JF, Murphey RD, Berghmans S, Mayhall EA, Traver D, Fletcher CD, Aster JC, Granter SR, Look AT, Lee C, Fisher DE, Zon LI.

Howard Hughes Medical Institute, Harvard Medical School, 300 Longwood Avenue, Boston, MA 02115, USA.

Melanoma is the most lethal form of skin cancer, and the incidence and mortality rates are rapidly rising. Epidemiologically, high numbers of nevi (moles) are associated with higher risk of melanoma . The majority of melanomas exhibit activating mutations in the serine/threonine kinase BRAF . BRAF mutations may be critical for the initiation of melanoma ; however, the direct role of BRAF in nevi and melanoma has not been tested in an animal model. To directly test the role of activated BRAF in nevus and melanoma development, we have generated transgenic zebrafish expressing the most common BRAF mutant form (V600E) under the control of the melanocyte mitfa promoter. Expression of mutant, but not wild-type, BRAF led to dramatic patches of ectopic melanocytes, which we have termed fish (f)-nevi. Remarkably, in p53-deficient fish, activated BRAF induced formation of melanocyte lesions that rapidly developed into invasive melanomas, which resembled human melanomas and could be serially transplanted. These data provide direct evidence that BRAF activation is sufficient for f-nevus formation, that BRAF activation is among the primary events in melanoma development, and that the p53 and BRAF pathways interact genetically to produce melanoma.

APPENDIX D

[CANCER RESEARCH 64, 7256–7262, October 15, 2004]

Targeted Expression of Human *MYCN* Selectively Causes Pancreatic Neuroendocrine Tumors in Transgenic Zebrafish

Hong Wei Yang,[1] Jeffery L. Kutok,[2] Nam Hyuk Lee,[1] Hui Ying Piao,[1] Christopher D. M. Fletcher,[2] John P. Kanki,[1] and A. Thomas Look[1]

[1]Department of Pediatric Oncology, Dana-Farber Cancer Institute, and [2]Department of Pathology, Brigham and Women's Hospital, Harvard Medical School, Boston, Massachusetts

ABSTRACT

The zebrafish model organism has been used extensively for studies of genetic pathways in development, indicating its potential applicability to cancer. Here we show that targeted expression of *MYCN* in cells of the pancreatic islet induces neuroendocrine carcinoma. Four transgenic fish developed abdominal tumors between 4 and 6 months of age, and histologic analysis revealed lobulated arrangements of neoplastic cells with expression of the *MYCN* transgene. The tumors also expressed insulin mRNA, and pancreatic exocrine cells and ducts were identified within the neoplasms, indicating a pancreatic origin for the tumor. Transmission electron microscopy revealed cytoplasmic, endocrine-dense core granules, analogous to those found in human neuroendocrine tumors. Our studies establish a zebrafish transgenic model of pancreatic neuroendocrine carcinoma, setting the stage to evaluate molecular pathways downstream of *MYCN* in this vertebrate forward genetic model system.

INTRODUCTION

The zebrafish system has been broadly used for elucidating genetic pathways in development (1–4). The zebrafish has also been shown to be a relevant vertebrate system to model human cancer, displaying many similarities in tumorigenic pathways, despite the evolutionary divergence of mammals and fish more than 300 million years ago (5, 6). The zebrafish (whose genome contains cell-cycle genes, tumor suppressor genes, and oncogenes found in humans and other mammals) has enormous potential as a vertebrate system in which to identify novel molecular pathways of oncogenesis, especially because zebrafish are prone to develop tumors (5, 7–11). Zebrafish have also played an important role as a vertebrate model system in carcinogenesis to determine environmental effects, genetic susceptibility, and environmental-genomic interactions (5, 12–14).

Recently, our laboratory has developed the first transgenic model of leukemia in the zebrafish, by expressing the murine *Myc* gene in developing thymocytes, under the control of the *Rag-2* promoter (6). Given the proven utility of the zebrafish system for forward genetic screens to dissect developmental pathways (1–4), it should be possible to find modifier genes that either accelerate or reduce the rate of onset of leukemia in these transgenic lines. The zebrafish system is also conducive to high-throughput target validation and drug screening, providing a crucial link between high-throughput *in vitro* assays and *in vivo* disease models (15).

MYC, MYCN, and MYCL are the three members of the Myc oncoprotein family with well-established roles in the pathogenesis of many human neoplastic diseases (16). *MYCN*, for example, is amplified and misexpressed in a variety of different tumors including ~25% of childhood neuroblastomas, where it signifies an adverse prognosis (17, 18), as well as in tumors of neuroectodermal origin, including medulloblastoma, retinoblastoma, astrocytoma, glioblastoma, rhabdomyosarcoma, and small-cell lung cancer (19–23).

In this study, we generated transgenic zebrafish by targeted expression of the human *MYCN* transgene under the control of a promoter that targets gene expression in pancreatic neuroendocrine β cells as well as in muscle cells and neurons. These transgenic fish selectively developed pancreatic β-cell tumors that express insulin mRNA and histologically resemble human pancreatic neuroendocrine carcinomas.

MATERIALS AND METHODS

Cloning of Zebrafish *myod* Gene (*z-myod*) Genomic DNA, Construction of Plasmids, and Microinjection of DNA into Zebrafish Embryos. A *z-myod* genomic PAC clone was isolated by screening a zebrafish PAC library with a *z-myod* cDNA probe. A 6-kb promoter fragment was then isolated from the *z-myod* PAC with *Apa*I and EcoR V and cloned into a pSK+ vector. The *z-myod–EGFP* construct was made by inserting the *EGFP* in frame with the ATG codon of the *z-myod* gene. The 258-bp core enhancer of the human *MYOD* gene (24) was cloned by PCR and then inserted at the 5′ end of the *z-myod* promoter construct (*zmyod-EGFP*; Fig. 1*A*) to make the core-*zmyod–EGFP* construct (Fig. 2*A*). The *z-myod–MYCN* and core-*zmyod–MYCN* constructs were generated by replacing the *EGFP* with the *MYCN* cDNA in the *zmyod-EGFP* and core-*zmyod–EGFP* constructs. The DNA for injection was released from vector by *Pvu*I digestion and then purified from the gel with a QIAEX II Gel Purification Kit (Qiagen Inc., Valencia, CA). The F0 mosaic fish were generated by injecting the linearized transgenes (100 ng/μL) into the cytoplasm of fertilized embryos at the one-cell stage.

Fish Maintenance and Embryonic Staging. Zebrafish were maintained and developmentally staged according to Westerfield *et al.* (25). Briefly, wild-type fish were mated, and the embryos were collected and grown in E3 medium (5 mmol/L NaCl, 0.17 mmol/L KCl, 0.4 mmol/L $CaCl_2$, and 0.16 mmol/L $MgSO_4$) at 28.5°C. Between 18 and 24 hours post-fertilization (hpf), embryos were transferred to E3 medium containing 0.003% 1-phenyl-2-thiourea to inhibit pigment formation and to prolong their optical transparency. Embryos were fixed at various stages of development in 4% paraformaldehyde at 4°C overnight. Fixed embryos were washed in PBS with 0.1% Tween 20 and stored in methanol at −20°C.

Whole-Mount *In situ* Hybridization. Digoxigenin- and fluorescein-labeled RNA probes were transcribed from linear cDNA constructs according to the manufacturer's instructions (Roche Molecular Biochemicals, Indianapolis, IN). Probes for zebrafish insulin, glucagon, and somatostatin were kindly provided by Dr. F. Argenton (Department of Biology, University of Padova, Padova, Italy). Probes were isolated by reverse transcription-PCR with primers based on the sequences in the National Center for Biotechnology Information database for chromogranin A (BM025152; primers: forward, 5′AACACCAGCAGCGCCTAATG; and reverse, 5′AGTCTTTAGGGAGGCTGGTC) and synaptophysin (BM958377; primers: forward, 5′CCGGAATCGAAGTGTTTTGT; and reverse, 5′GCTGGTAGCCCAAGTACAGG). Whole-mount *in situ* hybridization assays were done as described previously (26).

Paraffin Embedding and Sectioning. Euthanized fish were placed in 4% paraformaldehyde at 4°C for 4 days and then transferred to 0.25 mol/L EDTA (pH 8.0) for no less than 2 days. The fish were then dehydrated in alcohol, cleared in xylene, and infiltrated with paraffin. Tissue sections (4-μm thick) from paraffin-embedded tissue blocks were placed on charged slides, depar-

Received 3/22/04; revised 8/24/04; accepted 8/26/04.

Grant support: Claudia Adams Barr Awards for Innovative Cancer Research (H. Yang and A. Look) and NIH Grant NIH-P30CA6516.

The costs of publication of this article were defrayed in part by the payment of page charges. This article must therefore be hereby marked *advertisement* in accordance with 18 U.S.C. Section 1734 solely to indicate this fact.

Requests for reprints: A. Thomas Look, Department of Pediatric Oncology, Mayer 630, Dana-Farber Cancer Institute, Boston, MA 02115. Phone: (617) 632-5826; E-mail: thomas_look@dfci.harvard.edu.

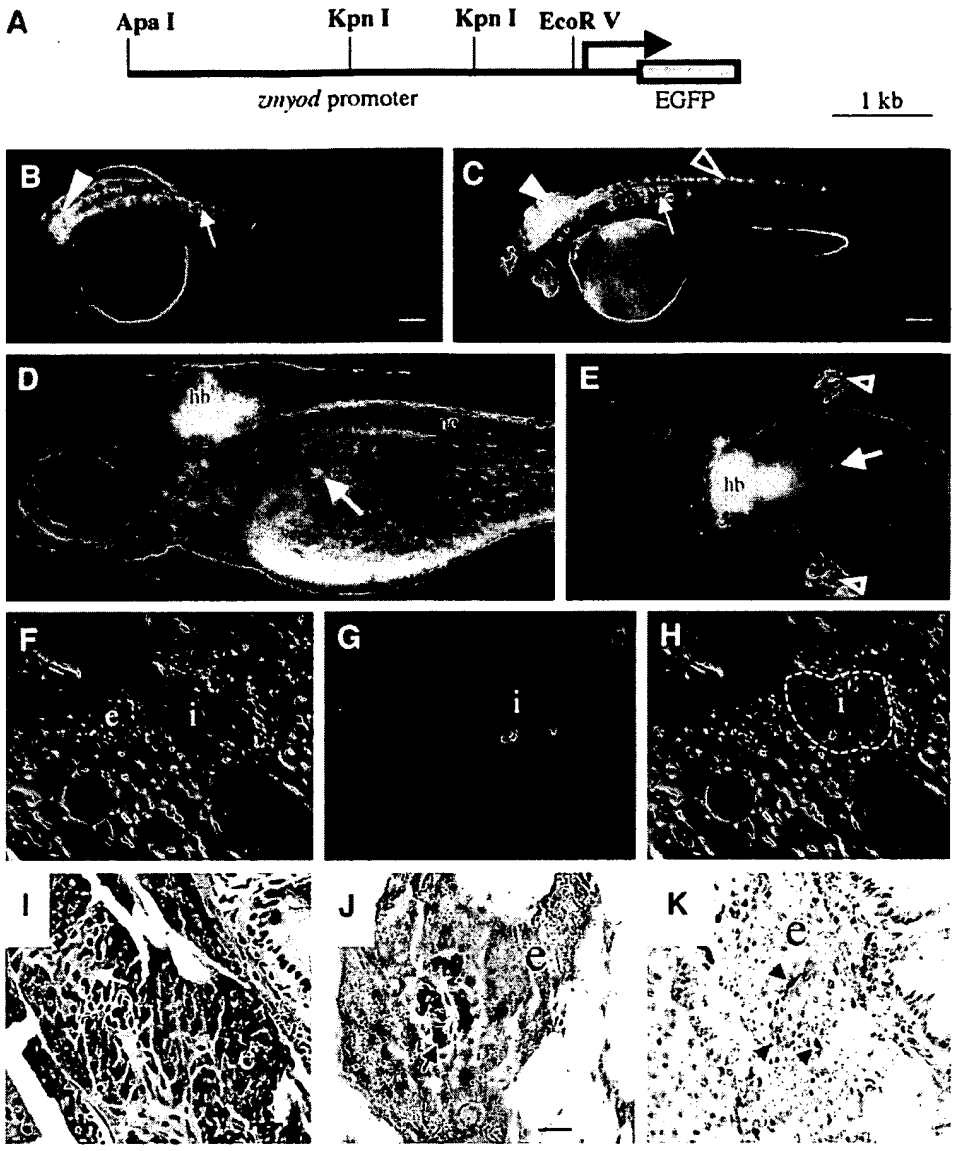

Fig. 1. EGFP expression in the *z-myod–EGFP* transgenic line. *A*. The *zmyod-EGFP* transgenic construct was made by fusing the EGFP coding sequence to a 6-kb promoter fragment of the *z-myod* gene. Zebrafish embryos microinjected at the one-cell stage began expressing EGFP as early as 6 hpf (data not shown). *B*. At 30 hpf, EGFP is expressed in the hindbrain (*arrowhead*) and notochord (*arrow*). *C*. At 48 hpf, EGFP is strongly expressed in the hindbrain (*arrowhead*), notochord (*arrow*), and neurons in the spinal cord (*open arrowhead*). *D* and *E*. EGFP is expressed in pancreatic islet cells (*arrow*) at 5 days post-fertilization (dpf), as shown in dorsolateral and dorsal views, respectively. Expression in the hindbrain and developing pectoral fins is indicated (*open arrowhead*). *F–H*, sagittal frozen section through the pancreatic islet of 5 dpf zebrafish (400×). *F*, bright field. *G*, EGFP fluorescence. *H*, merged view [exocrine cells (*e*) and islet cells (*i*) are indicated]. *I–K*, paraffin-embedded section through the pancreatic islet of the adult zebrafish. *I*, H&E stain. *J*, mRNA *in situ* hybridization with an insulin antisense riboprobe. *K*, immunohistochemical staining with an anti-GFP antibody (*dark brown cells, arrows*; Pancreatic islet cells (*arrows*) and exocrine cells (*e*) are indicated). (*hb*, hindbrain)

affinized in xylene, rehydrated through graded alcohol solutions, and stained with hematoxylin/eosin (H&E).

Immunohistochemistry. Immunohistochemical studies for green fluorescent protein (GFP) were done as described previously (6). Immunofluorescence for insulin was done on 10-μm frozen sections with anti-insulin K36aC10 (1:1,000; Sigma, St. Louis, MO), antiglucagon (1:100; Chemicon, Temecula, CA), and Cy3-conjugated antimouse IgG was used as secondary antibody. Confocal images were taken on a Zeiss LSM 510 microscope.

Electron Microscopy. Tumor tissue was fixed in a glutaraldehyde/paraformaldehyde mixture (2.5% glutaraldehyde; 2% paraformaldehyde) in 0.1 mol/L sodium cacodylate buffer (pH 7.4). After a brief rinse in 5% sucrose in 0.1 mol/L sodium cacodylate buffer (pH 7.4), tissues were post-fixed in osmium-S-collidine solution [1.33% osmium tetroxide in 0.066 mol/L S-collidine buffer (pH 7.4)] for 2 hours. The tissue was then dehydrated in graded EtOH solutions, cleared in propylene oxide, and infiltrated first in a 1:1 mixture of propylene oxide and Poly/Bed mixture for 60 minutes, followed by infiltration in undiluted Poly/Bed for 30 minutes. Semithin sections (1.0 μm) were stained with alkaline toluidine blue, and ultrathin sections were cut on an ultramicrotome, picked up on 200 mesh copper grids, and stained on the grid with saturated uranyl acetate solution for 15 minutes and 0.1 to 0.4% of lead citrate for 45 seconds. The grids were examined in a Jeol JEM 1010 electron microscope at 80 kV acceleration voltage. Images were recorded with an AMT digital camera.

RESULTS

Analysis of Zebrafish *z-myod* Promoter Sequences *In vivo*. In hopes of generating transgenic lines that express transgenes in muscle cell progenitors, we cloned 6.0 kb of genomic sequence upstream of the initiator codon of *z-myod* and fused these sequences to the gene encoding enhanced green fluorescence protein (EGFP; Fig. 1*A*). This transgene was microinjected into the cytoplasm of fifty fertilized zebrafish embryos (one-cell stage) to generate F0 mosaic fish. The F1 progeny of one of these fish expressed EGFP during embryogenesis, indicating germline transmission of the transgene. In this stable line, EGFP was expressed primarily in the interneurons of the hindbrain and spinal cord and lacked expression in the skeletal musculature (Fig. 1, *B–E*), indicating that the genomic sequences tested had promoter activity but lacked sequences required for expression in developing muscle cells. EGFP was also ectopically expressed in islet cells of the pancreas (Fig. 1, *D–K*).

Similar results have been obtained in the mouse, in that a minimal mouse *MyoD* promoter ectopically drives transgene expression in the brain and spinal cord. In the mouse, a 258-bp core enhancer, located 20 kb upstream of the initiator codon, was identified that is required

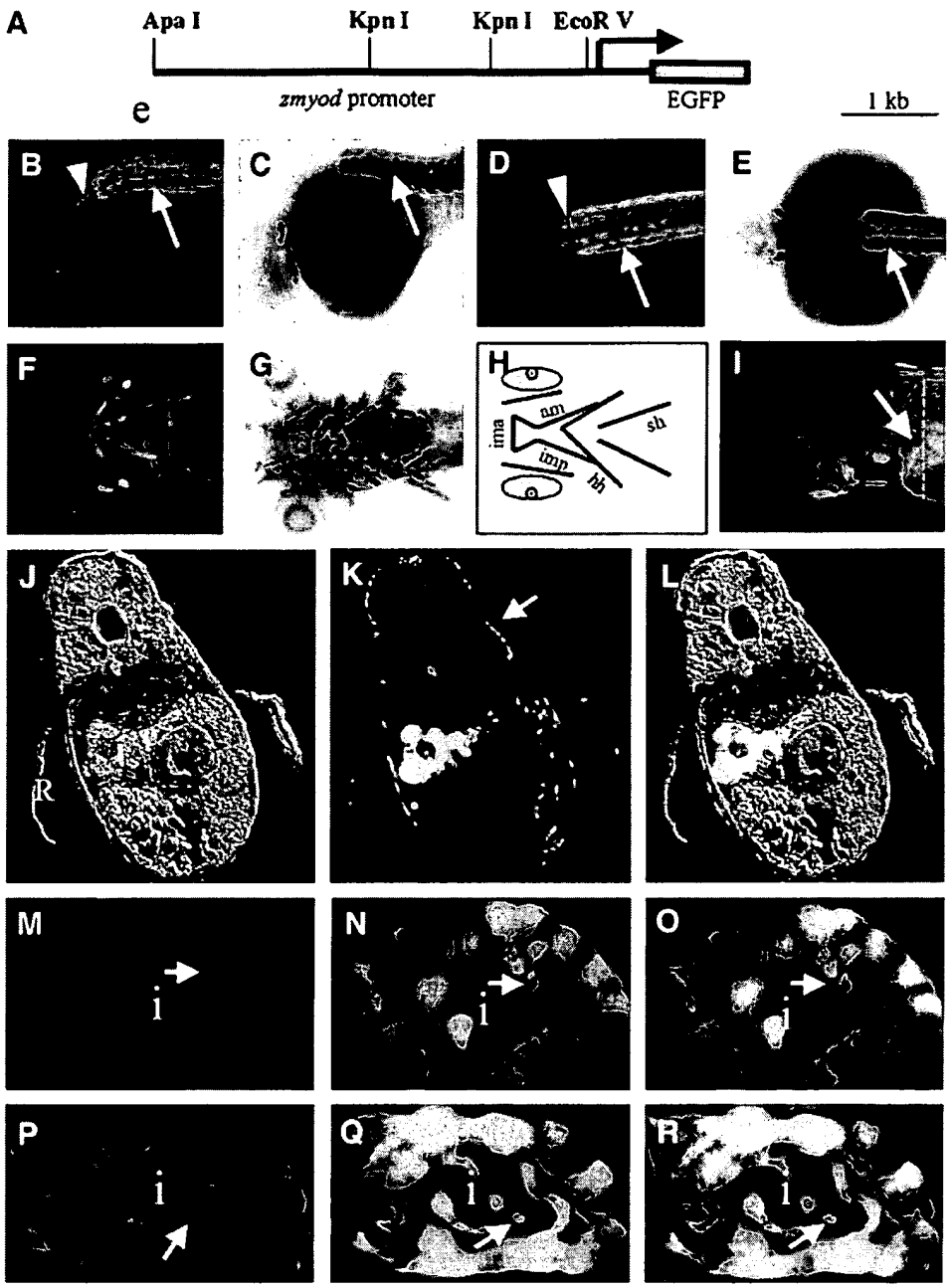

Fig. 2. Gene expression patterns in the core-*zmyod*–EGFP transgenic line. *A*. The transgenic construct was made by fusing the human *MYOD* 258-bp upstream core enhancer to the 5′ end of the *zmyod*-EGFP construct (Fig. 1*A*). *B*. Lateral views at 30 hpf, showing EGFP expression (green cells) in the spinal cord (*arrowhead*) and somites (*arrow*). *B–I*, anterior is to the left. *C*, endogenous *z-myod* expression detected in somitic muscle cells by mRNA *in situ* hybridization (*arrow*). *D* and *E*, dorsal views of the zebrafish in *panels B* and *C*, respectively. *F*, ventral view of the head at 5 dpf, showing high levels of expression of EGFP in the jaw muscles. *G*, ventral view at 5 dpf, showing endogenous *z-myod* expression, by mRNA *in situ* hybridization. *H*, schematic diagram showing the jaw muscles evident in *F* and *G*. *I*, lateral view of EGFP expression in the head and upper abdomen of a 5 dpf zebrafish (*arrow*, pancreatic islet). *J–L*, frozen cross section through the pancreas at 5 dpf. *J*, bright-field view (*e*, exocrine cells; *i*, islet are indicated; *R*, right side). *K*, EGFP fluorescence (superficial slow muscle, *arrow*); and *L*, merged view of sections cut along the plane shown by the *dashed lines* in *panel I*. *M–O*, colocalization of insulin and EGFP in islet cells. *M*, immunofluorescence of insulin in an islet cell (red cells). *N*, EGFP fluorescence. *O*, merged view, *arrows* indicate a cell expressing insulin and EGFP. *P–R*, colocalization of glucagon and EGFP in islet cells. *P*, immunofluorescence analysis of glucagons expression (red cells). *Q*, EGFP fluorescence. *R*, merged view: *arrows* indicate a cell expressing glucagon and EGFP. (*ima*, intermantibularis anterior; *imp*, intermantibularis posterior; *am*, adductor mandibulae; *hh*, hypohyroideus; *sh*, sternalhyoideus)

for expression in muscle cells (24, 27, 28). Rather than search for an analogous element in the zebrafish gene, we cloned the human *MYOD* 258-bp core enhancer upstream of the 6.0-kb zebrafish promoter sequence generating a construct, core-*zmyod–EGFP* (Fig. 2*A*). Eighty zebrafish embryos were injected with this construct, grown to adulthood, and the offspring of two of these fish were found to express EGFP, indicating germline transmission of the transgene. These lines showed EGFP expression in the muscle cells of the somites at 24 hpf and in the jaw muscles beginning at 72 hpf. The pattern of transgene expression in muscle cells with this construct was nearly identical to the pattern of expression of the endogenous *z-myod* gene, as detected by whole-mount *in situ* hybridization assay with an antisense *z-myod* riboprobe (Fig. 2, *B–H*). However, expression levels of the transgene in the hindbrain, spinal cord, and pancreatic islet were similar to those previously obtained with the 6.0-kb zebrafish genomic fragment, indicating that although the human *MyoD* core enhancer sequences were able to activate transgene expression by muscle cells, the ectopic expression in neural cells, and the pancreas was not suppressed. (Fig. 2, *D* and *I–L*). Although EGFP expression is most prominent in the exocrine pancreas, expression was also evident in a subset of the endocrine cells (Fig. 2, *K* and *L*). To specifically document EGFP expression by pancreatic endocrine cells in this line, we showed that the core z-myod promoter construct (EGFP; *green*) is coexpressed with insulin (Cy3; *red*) in a subset of pancreatic endocrine cells (Fig. 2, *M–O*), and with glucagon (Cy3; *red*), also in a subset of these cells (Fig. 2, *P–R*).

Neuroendocrine Tumors in *MYCN* Transgenic Zebrafish. To generate *MYCN* transgenic fish, we fused the human *MYCN* oncogene to either the *z-myod* or core-*zmyod* promoter sequences. The linearized transgenic constructs were microinjected into the cytoplasm of one-cell stage embryos to generate 250 F0 mosaic fish. Five of these mosaic transgenic fish developed tumors between 3 and 6 months of

Table 1 *Characteristics of tumors in MYCN mosaic transgenic zebrafish*

					In situ hybridization					
Case	Promoter	Oncogene	Age	Site	MYCN	chr	syn	ins	glu	soma
1	z-myoD	*MYCN*	5 months	abd	+	−	−	+	−	−
2	z-myoD	*MYCN*	6 months	abd	+	−	−	+	−	−
3	core-z-myoD	*MYCN*	3 months	head	+	−	+	−	−	−
4	core-z-myoD	*MYCN*	5 months	abd	+	−	−	+	+	−
5	core-z-myoD	*MYCN*	6 months	abd	+	−	−	+	−	−

Abbreviations: abd, abdomen; syn, synaptophysin; ins, insulin; glu, glucagon; soma, somatostatin.

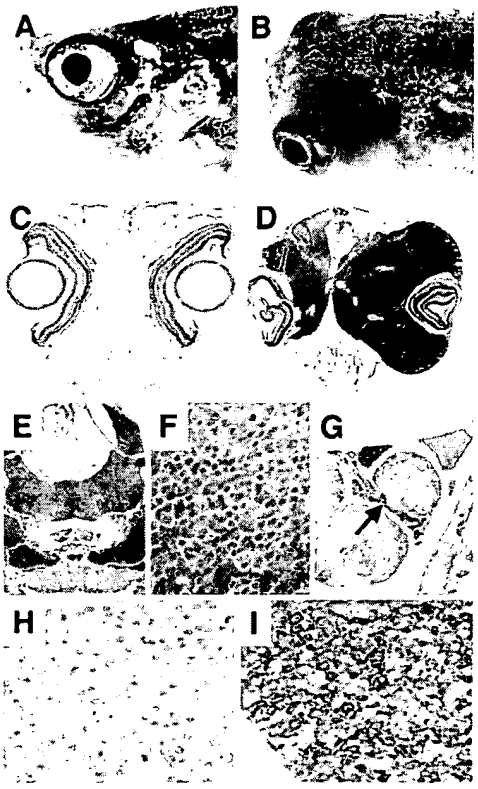

Fig. 3. Pathological analysis of an intracranial tumor arising in *MYCN* transgenic fish (Case 3, Table 1). *A* and *B*, gross morphology of adult zebrafish. *A*, wild-type control. *B*, core-*zmyod–MYCN* transgenic fish showing massive exopthlamos. *C–G*, H&E staining of paraffin cross sections. *C*, wild-type. *D*. Core-*zmyod–MYCN* transgenic fish, showing tumor cells effacing the retro-orbital space, leaving a clear boundary between tumor cells and surrounding tissues (20× magnification). *E*. Cross section through the hindbrain reveals the tumor was originating within the cranial cavity. *F*, magnified view of tumor cells (400× magnification). *G*, section through the pancreas (*arrow*) showing normal tissue morphology. *H*, mRNA *in situ* hybridization with a sense, control RNA probe. *I*, mRNA *in situ* hybridization with an antisense RNA probe for the human *MYCN* gene, reveals high levels of *MYCN* expression (*dark staining*).

age. In two cases, *MYCN* was driven by the *z-myod* promoter and in three cases, *MYCN* was driven by the core-*zmyod* promoter (Table 1). One of the fish (Case 3) was sacrificed when it developed exopthalmos at three months of age, and histologic analysis of tissues underlying the eye indicated an epithelial tumor with neuroendocrine differentiation (Fig. 3). The tumor cells expressed the *MYCN* transgene, as indicated by *in situ* hybridization assay with an antisense *MYCN* riboprobe (Fig. 3*I*).

The remaining four transgenic fish developed abdominal tumors between 4 and 6 months of age (Fig. 4, *A–D*). The tumors were anatomically distinct from the liver, and histologic analysis of paraffin sections revealed an encapsulated, lobulated, or nested arrangement of neoplastic-appearing cells. These cells were polygonal in shape and possessed a high nuclear/cytoplasmic ratio, distinct nucleoli and small to moderate amounts of eosinophilic cytoplasm. Delicate fibrovascular stromal tissue gave some tumors a clearly nested or nodular appearance. The mitotic rate was low, and single cell necrosis was minimal; however, the expansile tumors were locally invasive into adjacent nonpancreatic tissue (Fig. 4*H*). Small residual aggregates of normal-appearing pancreatic exocrine cells and ducts were identified within the neoplasm, which together with the histologic features, suggested a pancreatic origin for the tumor (Fig. 4, *E–G*). To aid in confirming this histologic evaluation, transmission electron microscopy was done on tissues from two tumors. In one of the two tumors, well-granulated tumor cells were identified with solid, round to

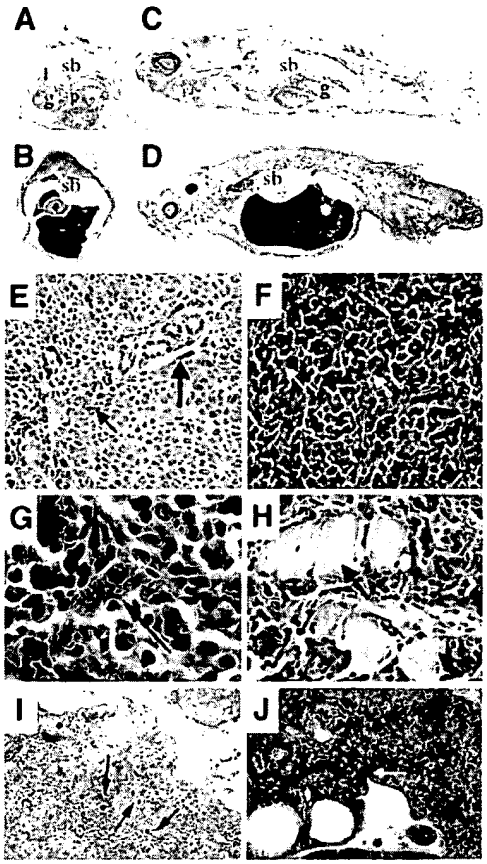

Fig. 4. Histologic analysis of human *MYCN*-induced pancreatic tumors in zebrafish. *A–D*, 20× magnification of H&E-stained paraffin sections of adult zebrafish. *A* and *B*, cross section. *C* and *D*, sagittal section. *A* and *C*, wild-type. *B* and *D*, two different transgenic fish. *E*. The 400× magnification of *B*, pancreatic duct (*bold arrow*), and pancreatic cells (*small pink cells, arrow*) were identified within the tumor tissue. *F*, 400× magnification of *D*, normal pancreatic cells (*small pink cells, arrows*). *G–H*, histology of tumors in core-*zmyod–MYCN* transgenic fish (400× original magnification). *G*. Pancreatic cells (*arrow*) are distributed through the tumor tissue. *H*, Expansile tumors were locally invasive into adjacent nonpancreatic tissue and musculature (*arrows*). *I*, electron microscopic image of tumor tissue shown in *G*, *arrows* indicate the secretory granules in the cytoplasm of the tumor cells. *J*. Electron microscopic image of tumor tissue shown in *H*; the tumor showed some characteristics of epithelial cells, the *arrow* indicates the intermembranous tight junctions between two tumor cells. (*g*, gut; *l*, liver; *p*, pancreas; *sb*, swim bladder; *T*, tumor)

slightly irregular haloed cytoplasmic neurosecretory granules of low to intermediate density, suggestive of those seen in human neuroendocrine tumors (Fig. 4*I*). In addition, intermembrane tight junctions of epithelial cells were evident (Fig. 4*J*).

To additionally establish the endocrine nature of these tumors, *in situ* hybridization assays were done with mRNA probes encoding hormones, the expression levels of which are used as markers for neuroendocrine tumors (29). Synaptophysin is an integral membrane protein of small synaptic vesicles in brain and endocrine cells (30). Insulin is synthesized by the β cells of pancreatic islets (31). Glucagon is a 29-amino acid pancreatic hormone that counteracts the glucose-lowering action of insulin by stimulating glycogenolysis and gluconeogenesis (32). Chromogranin A is secreted by a great variety of peptide-producing endocrine neoplasms: pheochromocytoma, parathyroid adenoma, medullary thyroid carcinoma, carcinoids, oat-cell lung cancer, pancreatic islet-cell tumors, and aortic-body tumor (33). Somatostatin is widely distributed throughout the body and is an important regulator of endocrine and nervous system function (34). The tumor cells of Case 3 expressed zebrafish synaptophysin (*z-syn*) RNA but not zebrafish insulin (*z-ins*), glucagon (*z-glu*), chromogranin (*z-chr*), or somatostatin (*z-soma*; Table 1; data not shown). The tumor cells of Cases 1, 2, 4, and 5 all expressed both high levels of human *MYCN* mRNA (Fig. 5, *A* and *B*) as well as zebrafish insulin mRNA (Fig. 5, *C–F*). One fish (Table 1, Case 4) also revealed slightly positive staining of glucagon (*z-glu*; data not shown). We did not detect expression of zebrafish chromogranin (*z-chr*) or somatostatin (*z-soma*; Table 1; data not shown). Taken together, our studies indicate that the *z-myod* promoter-driving MYCN expression in the zebrafish causes the development of neuroendocrine epithelial tumors that are classified as neuroendocrine carcinomas, with anatomic and gene expression findings in four of the five tumors, suggesting origins in insulin-producing islet cells of the pancreas.

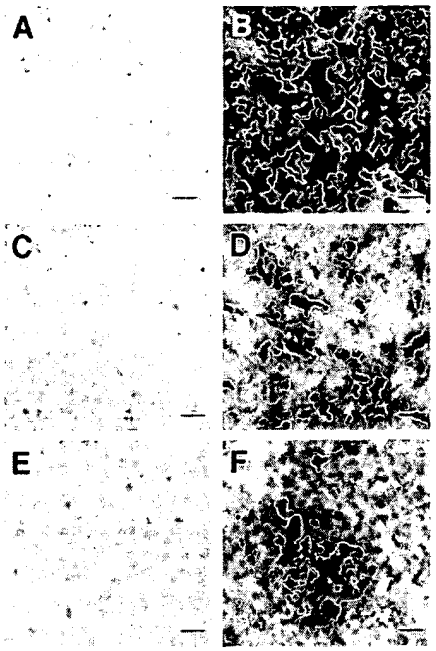

Fig. 5. The mRNA *in situ* hybridization analysis of human *MYCN*-induced pancreatic tumors in transgenic zebrafish (400× original magnification). *A* and *B*, *MYCN* mRNA *in situ* hybridization. *A*, mRNA *in situ* hybridization with a sense, control RNA. *B*, mRNA *in situ* hybridization with an antisense RNA probe for the human *MYCN* gene, revealed high levels of tumor-cell–specific expression of the *MYCN* transgene. *C–F*, insulin mRNA *in situ* hybridization analysis. *C* and *E*, mRNA *in situ* hybridization with sense control RNA probe. *D* and *F*, mRNA *in situ* hybridization with an antisense RNA probe for the zebrafish *insulin* gene, revealed high levels of expression of the gene by the tumor cells.

At one year of age, all of the F0 *MYCN* transgene-injected fish were sacrificed, and serial transverse sections were stained with H&E and analyzed histologically for the presence of tumors. We did not detect any additional neuroendocrine tumors or any other type of tumor in this analysis, indicating that although the zmyod promoters drive transgene expression in other organs, the misexpression of MYCN does not initiate cancer in other tissue types. It is possible that in tissues other than the endocrine pancreas, the *zmyod* promoters drive the expression of MYCN in cells that have differentiated further, which lack self-renewal capacity and thus cannot form malignant tumors.

DISCUSSION

We have developed a zebrafish transgenic model system for pancreatic neuroendocrine carcinoma. In humans, pancreatic neuroendocrine tumors include both benign and malignant epithelial neoplasms that show evidence of endocrine cell differentiation (35). These tumors often secrete active hormones, such as insulin or glucagon, and patients may suffer from pronounced paraneoplastic syndromes because of the overproduction of these hormones. Insulin-secreting β-islet cell tumors are the most common type of pancreatic neuroendocrine neoplasms in man. The locally invasive growth pattern identified in our zebrafish tumors favors a malignant rather than a benign lesion.

Relatively little is known about the genetic events that occur during the initiation and progression of pancreatic β-cell neoplasms in humans. However, several observations suggest that activation of the proto-oncogenes, *MYC* and *RAS* and overexpression of transforming growth factor α (*TGF-α*) often occur with malignant progression and that mutations inactivating the p53 tumor suppressor protein are common (36, 37). Pavelic *et al.* (36, 37) have proposed that *MYC* activation appears to be an early event in human β-cell tumor progression, because it is expressed at higher levels in β-cell hyperplastic islets than in normal islet cells and at even higher levels in benign and malignant tumors.

We used an upstream fragment of the zebrafish *z-myod* gene as the promoter to generate transgenic animal expressing the human *MYCN* oncogene. Mammalian *MyoD* promoters have a very complicated structure. A 258-bp enhancer located 20 kb upstream of the transcriptional start site is necessary to drive transgene expression in muscle cell progenitors in the mouse, because a minimal promoter fragment, lacking this upstream motif, primarily mediates neuronal expression (24, 27, 28). Our results in zebrafish were quite similar, in that a 6-kb minimal promoter fragment of *z-myod* resulted in EGFP expression that was most pronounced in the hindbrain, spinal cord, and pancreatic islets (Fig. 1, *A* and *B*). These results suggest that the 6-kb promoter of *z-myod* has activity but lacks the elements necessary to initiate muscle expression, as had been previously observed for the mouse minimal promoter of MyoD in transgenic mice (24, 27). In an attempt to obtain expression in zebrafish muscle cells, we tested the 258-bp core enhancer of the human *MYOD* gene upstream of our *z-myod* promoter fragment, forming a human-zebrafish chimeric promoter. Interestingly, this chimeric promoter functioned well to drive high levels of transgene expression in muscle cells of the zebrafish, both when transiently injected at the one-cell stage and also in the progeny of two different EGFP-expressing stable lines. Muscle cells in both the trunk and the craniofacial regions expressed high levels of EGFP. However, the 258-bp core enhancer of the human *MYOD* gene did not prevent the ectopic expression of EGFP in neuronal and pancreatic islet cells in our transgenic lines, suggesting that our chimeric construct still lacks repressor sequence motifs that commonly prevent expression of the endogenous *z-myod* gene in these tissues. Our

success in using human enhancer elements to drive muscle expression in zebrafish suggests evolutionary conservation of regulatory enhancer sequence elements and *trans*-acting transcription factors between these two species and raises the possibility that the zebrafish system could be used to help identify and analyze the sequence motifs and transacting factors, the homologues of which perform similar roles during mammalian development.

The c-*Myc* proto-oncogene is implicated in pancreatic β-cell proliferation in tumorigenesis and may contribute to apoptosis of the same cells in diabetes (38). Although the vast majority of functional and transgenic studies of islet cell tumors have focused on the c-Myc protein, N-Myc functions in a very similar manner in a number of cell culture assays (39, 40). Indeed, when the coding region of the mouse c-*Myc* gene was replaced with the *N-Myc* coding sequence by homologous recombination, the resulting homozygous knock-in mice, in which the *c-Myc* promoter drives the synthesis of *N-Myc* mRNA instead of *c-Myc* mRNA, were viable and appeared normal, indicating that the N-Myc protein can functionally replace c-Myc if it is appropriately regulated (41). β-cell tumors that express insulin mRNA and histologically resemble human pancreatic endocrine carcinomas have been produced by transgenic expression of c-Myc, indicating the importance of the Myc pathway in the molecular pathogenesis of pancreatic neuroendocrine carcinoma (42). Studies in transgenic mice have shown that Myc activation initially promotes both proliferation and apoptosis in pancreatic β cells and that tumors arise when the apoptosis pathway is suppressed, indicating the need for at least two mutational events before tumors arise (42). Studies with a conditional c-Myc allele also showed that Myc expression is required not only for initiation for the tumor but also to maintain the neoplastic phenotype of established tumors (42). More recently, Lewis *et al.* (43) have generated a mouse model for pancreatic cancer through the somatic delivery of oncogene-bearing avian retroviruses to mice that express TVA, the receptor for avian leukosis sarcoma virus subgroup A (ALSV-A), under the control of the elastase promoter. Infection of elastase-*tv-a* transgenic mice, either wild-type or null for the *Ink4a/Arf* locus, with viruses encoding mouse polyoma virus middle T antigen induced highly penetrant acinar and ductal tumors. In contrast, infection of elastase-*tv-a*, *Ink4a/Arf* null mice with viruses encoding the c-Myc oncoprotein led to the formation of pancreatic endocrine tumors exclusively, indicating the importance of Myc in the tumorigenesis of pancreatic endocrine tumors (43).

We were surprised that we did not recover rhabdomyosarcoma in transgenic fish expressing *MYCN* driven by the core-*zmyod* promoter, because we observed high levels of expression of GFP in embryonic muscle cells with this promoter, and *MYCN* is amplified and overexpressed in most human rhabdomyosarcomas (44). There are several possibilities to explain this observation. Although expressed at high levels in muscle cells, core-zmyod may not drive expression in muscle stem cells with the capacity for self-renewal, thus preventing the acquisition of additional mutations needed for the formation of a malignant tumor. Alternatively, high levels of *MYCN* expression driven by this promoter may lead to apoptosis of muscle stem cells that integrate the transgene, preventing transformation. Lastly, it remains possible that MYCN overexpression is not a rate-limiting step in rhabdomyosarcoma and that other mutations are needed before developing myoblasts are susceptible to MYCN-induced transformation.

One advantage of the zebrafish model lies in its ability to accommodate large-scale "forward-genetic" screens to identify modifier genes. For such screens we will need to establish a stable transgenic line expressing *MYCN*, which we have not thus far recovered, although we were able to generate stable lines expressing EGFP alone from both promoters. A likely possibility is that the promoter we are using drives MYCN expression in germ cells that integrate the transgene, which is toxic to them. We are now injecting a Cre-Lox conditional transgene to establish stable lines that only express EGFP until MYCN is induced through the controlled expression of Cre. This system has worked with other promoters, so we feel confident that it will ultimately be successful.

Once forward-genetic screens become possible in our system, germline mutations induced by either ethyl-nitrosourea or retroviral integration into large numbers of mutagenized transgenic zebrafish will be analyzed for mutations that accelerate or retard the rate of development of Myc-induced tumors. For example, mutations that inactivate tumor suppressor genes and accelerate the onset of clonal tumors should be identified, because the mutant fish would carry inactivating mutations of single tumor suppressor alleles throughout development, increasing the likelihood of acquiring inactivating mutations or deletions affecting both alleles of the same gene. In addition, mutations identified in unbiased screens that delay or prevent tumorigenesis may provide insight into human homologues that could serve as targets for the development of small molecule inhibitors.

ACKNOWLEDGMENTS

We thank Janice Williams, Vuong Nguyen, and Coneen Ford for expert technical assistance, Doris Dodson for manuscript preparation, and George Kourkoulis, Jessica Vinokur, and Walt Saganic for excellent zebrafish care and maintenance. We also thank Dr. Argenton, who kindly provided us with the probes for zebrafish insulin, glucagon, and somatostatin.

REFERENCES

1. Driever W, Solnica-Krezel L, Schier AF, et al. A genetic screen for mutations affecting embryogenesis in zebrafish. Development (Camb) 1996;123:37–46.
2. Haffter P, Granato M, Brand M, et al. The identification of genes with unique and essential functions in the development of the zebrafish, Danio rerio. Development (Camb) 1996;123:1–36.
3. Peterson RT, Link BA, Dowling JE, Schreiber SL. Small molecule developmental screens reveal the logic and timing of vertebrate development. Proc Natl Acad Sci USA 2000;97:12965–9.
4. Peterson RT, Mably JD, Chen JN, Fishman MC. Convergence of distinct pathways to heart patterning revealed by the small molecule concentramide and the mutation heart-and-soul. Curr Biol 2001;11:1481–91.
5. Amatruda JF, Shepard JL, Stern HM, Zon LI. Zebrafish as a cancer model system. Cancer Cell 2002;1:229–31.
6. Langenau DM, Traver D, Ferrando AA, et al. Myc-induced T cell leukemia in transgenic zebrafish. Science (Wash DC) 2003;299:887–90.
7. Inohara N, Nunez G. Genes with homology to mammalian apoptosis regulators identified in zebrafish. Cell Death Differ 2000;7:509–10.
8. Langenau DM, Palomero T, Kanki JP, et al. Molecular cloning and developmental expression of Tlx (Hox11) genes in zebrafish (Danio rerio). Mech Dev 2002;117: 243–8.
9. Liu TX, Zhou Y, Kanki JP, et al. Evolutionary conservation of zebrafish linkage group 14 with frequently deleted regions of human chromosome 5 in myeloid malignancies. Proc Natl Acad Sci USA 2002;99:6136–41.
10. Kalev-Zylinska ML, Horsfield JA, Flores MV, et al. Runx1 is required for zebrafish blood and vessel development and expression of a human RUNX1-CBF2T1 transgene advances a model for studies of leukemogenesis. Development (Camb) 2002;129: 2015–30.
11. Smolowitz R, Hanley J, Richmond H. A three-year retrospective study of abdominal tumors in zebrafish maintained in an aquatic laboratory animal facility. Biol Bull 2002;203:265–6.
12. Walker WW, Manning CS, Overstreet RM, Hawkins WE. Development of aquarium fish models for environmental carcinogenesis: an intermittent-flow exposure system for volatile, hydrophobic chemicals. J Appl Toxicol 1985;5:255–60.
13. Spitsbergen JM, Tsai HW, Reddy A, et al. Neoplasia in zebrafish (Danio rerio) treated with N-methyl-N'-nitro-N-nitrosoguanidine by three exposure routes at different developmental stages. Toxicol Pathol 2000;28:716–25.
14. Spitsbergen JM, Tsai HW, Reddy A, et al. Neoplasia in zebrafish (Danio rerio) treated with 7,12-dimethylbenz[a]anthracene by two exposure routes at different developmental stages. Toxicol Pathol 2000;28:705–15.
15. Rubinstein AL. Zebrafish: from disease modeling to drug discovery. Curr Opin Drug Discov Devel 2003;6:218–23.
16. Nesbit CE, Tersak JM, Prochownik EV. MYC oncogenes and human neoplastic disease. Oncogene 1999;18:3004–16.

17. Brodeur GM, Seeger RC, Schwab M, Varmus HE, Bishop JM. Amplification of N-myc in untreated human neuroblastomas correlates with advanced disease stage. Science (Wash DC) 1984;224:1121–4.
18. Seeger RC, Brodeur GM, Sather H, et al. Association of multiple copies of the N-myc oncogene with rapid progression of neuroblastomas. N Engl J Med 1985;313:1111–6.
19. Wong AJ, Ruppert JM, Eggleston J, et al. Gene amplification of c-myc and N-myc in small cell carcinoma of the lung. Science (Wash DC) 1986;233:461–4.
20. Garson JA, McIntyre PG, Kemshead JT. N-myc amplification in malignant astrocytoma. Lancet 1985;2:718–9.
21. Garson JA, Clayton J, McIntyre P, Kemshead JT. N-myc oncogene amplification in rhabdomyosarcoma at release. Lancet 1986;1:1496.
22. Garson JA, Pemberton LF, Sheppard PW, et al. N-myc gene expression and oncoprotein characterisation in medulloblastoma. Br J Cancer 1989;59:889–94.
23. Lee WH, Murphree AL, Benedict WF. Expression and amplification of the N-myc gene in primary retinoblastoma. Nature (Lond) 1984;309:458–60.
24. Goldhamer DJ, Faerman A, Shani M, Emerson CP Jr. Regulatory elements that control the lineage-specific expression of myoD. Science (Wash DC) 1992;256: 538–42.
25. Westerfield M, Doerry E, Kirkpatrick AE, Driever W, Douglas SA. An on-line database for zebrafish development and genetics research. Semin Cell Dev Biol 1997;8:477–88.
26. Bennett CM, Kanki JP, Rhodes J, et al. Myelopoiesis in the zebrafish, Danio rerio. Blood 2001;98:643–51.
27. Goldhamer DJ, Brunk BP, Faerman A, et al. Embryonic activation of the myoD gene is regulated by a highly conserved distal control element. Development (Camb) 1995;121:637–49.
28. Kucharczuk KL, Love CM, Dougherty NM, Goldhamer DJ. Fine-scale transgenic mapping of the MyoD core enhancer: MyoD is regulated by distinct but overlapping mechanisms in myotomal and non-myotomal muscle lineages. Development (Camb) 1999;126:1957–65.
29. Tomita T. New markers for pancreatic islets and islet cell tumors. Pathol Int 2002; 52:425–32.
30. Redecker P, Grube D. [Synaptophysin in the nervous system and endocrine cells]. Acta Histochem Suppl 1992;42:33–8.
31. Hartroft WS, Wrenshall GA. Correlation of beta-cell granulation with extractable insulin of the pancreas; studies in adult human diabetics and nondiabetics. Diabetes 1955;4:1–7.
32. Jiang G, Zhang BB. Glucagon and regulation of glucose metabolism. Am J Physiol Endocrinol Metab 2003;284:E671–8.
33. O'Connor DT, Deftos LJ. Secretion of chromogranin A by peptide-producing endocrine neoplasms. N Engl J Med 1986;314:1145–51.
34. Reichlin S. Secretion of somatostatin and its physiologic function. J Lab Clin Med 1987;109:320–6.
35. Wick MR, Graeme-Cook FM. Pancreatic neuroendocrine neoplasms: a current summary of diagnostic, prognostic, and differential diagnostic information. Am J Clin Pathol 2001;115(Suppl):S28–45.
36. Pavelic K, Hrascan R, Kapitanovic S, et al. Molecular genetics of malignant insulinoma. Anticancer Res 1996;16:1707–17.
37. Pavelic K, Hrascan R, Kapitanovic S, et al. Multiple genetic alterations in malignant metastatic insulinomas. J Pathol 1995;177:395–400.
38. Pelengaris S, Khan M. Oncogenic co-operation in beta-cell tumorigenesis. Endocr Relat Cancer 2001;8:307–14.
39. Aubry S, Charron J. N-Myc shares cellular functions wiht c-Myc. DNA Cell Biol 2000;19:353–64.
40. Mukherjee B, Morgenbesser SD, DePinho RA. Myc family oncoproteins function through a common pathway to transform normal cells in culture: cross-interference by Max and trans-acting dominant mutants. Genes Dev 1992;6:1480–92.
41. Malynn BA, de Alboran IM, O'Hagan RC, et al. N-myc can functionally replace c-myc in murine development, cellular growth, and differentiation. Genes Dev 2000;14:1390–9.
42. Pelengaris S, Khan M, Evan GI. Suppression of Myc-induced apoptosis in beta cells exposes multiple oncogenic properties of Myc and triggers carcinogenic progression. Cell 2002;109:321–34.
43. Lewis BC, Klimstra DS, Varmus HE. The c-myc and PyMT oncogenes induce different tumor types in a somatic mouse model for pancreatic cancer. Genes Dev 2003;17:3127–38.
44. Toffolatti L, Frascella E, Ninfo V, et al. MYCN expression in human rhabdomyosarcoma cell lines and tumour samples. J Pathol 2002;196:450–8.

APPENDIX E

The *pu.1* promoter drives myeloid gene expression in zebrafish

Karl Hsu, David Traver, Jeffery L. Kutok, Andreas Hagen, Ting-Xi Liu, Barry H. Paw, Jennifer Rhodes, Jason N. Berman, Leonard I. Zon, John P. Kanki, and A. Thomas Look

PU.1 is a member of the Ets family of transcription factors and plays an essential role in the development of both myeloid and lymphoid cells. To examine zebrafish *pu.1 (zpu.1)* expression in subpopulations of blood cells during zebrafish development, we linked a 9-kb zebrafish genomic fragment upstream of the *zpu.1* initiator codon to green fluorescent protein (GFP) and microinjected this construct to generate stable transgenic lines. GFP-positive fluorescent myeloid precursors were observed migrating from the anterolateral mesoderm in living embryos from 16 to 28 hours after fertilization (hpf) in a pattern that overlaps the expression pattern of endogenous *zpu.1* mRNA. Analysis of larval histologic sections revealed GFP-expressing hematopoietic cells in the developing zebrafish kidney. Flow cytometric analysis of cells from adult whole kidney marrow revealed 2 discrete subpopulations of GFP-positive cells, which after cell sorting exhibited either myeloid or early lymphoid morphology. Thus, the zebrafish *zpu.1* promoter fragment used here is capable of driving reporter gene expression in subsets of embryonic and adult hematopoietic cells. These transgenic lines will be useful to dissect the cellular and molecular control of myeloid cell differentiation, and this promoter fragment may prove useful in the development of zebrafish models of acute myeloid leukemia. (Blood. 2004;104:1291-1297)

Introduction

PU.1 is an Ets family transcription factor that plays an essential role in the development of both myeloid (granulocytes and monocytes/macrophages) and lymphoid cells.[1,2] Numerous studies of both human and murine tumor-derived cell lines and tissue samples have shown that PU.1 expression is restricted to hematopoietic cell lineages.[1-4] Studies of the promoter and enhancer sequences of a number of genes expressed by hematopoietic cells have defined PU.1-dependent regulatory elements, including components of the B-cell receptor and an array of adhesion molecules, growth factor receptors, and lysozymal enzymes expressed by myeloid cells.[5]

During hematopoiesis, PU.1 is up-regulated with myeloid and down-regulated with erythroid commitment.[6] In one PU.1-deficient mouse, embryos die in late gestation and exhibit an array of functional deficiencies in macrophages, granulocytes, and progenitors of B and T lymphocytes.[7] Another PU.1-deficient mouse is able to produce live pups that die soon after birth from septicemia.[8] These mice also have impaired myeloid development and lack B lymphocytes. Several recent studies have shown that PU.1 blocks erythroid differentiation by directly antagonizing GATA-1 activity.[9,10] The PU.1 promoter is regulated by PU.1 itself in an autoregulatory loop, and CCAAT/enhancer-binding protein α (C/EBPα) can induce PU.1 gene expression, suggesting a direct role for both proteins in the regulation of the PU.1 gene.[11] Overexpression of PU.1 in transgenic mice driven by the spleen focus-forming virus (SFFV) long-terminal-repeat (LTR) results in erythroleukemia.[12]

Analysis of the murine PU.1 promoter has shown that as little as 334 bp of the PU.1 promoter confers myeloid-specific gene expression in transient transfection assays.[13,14] However, this genomic fragment, as well as a longer fragment extending up to 2.1 kb, was unable to drive reporter gene expression in multiple lines of transgenic mice (D.G. Tenen, oral communication, January 2001). Recently, transgenic mice have been generated using a 91-kb murine PU.1 genomic DNA fragment to direct reporter gene expression in a pattern similar to that observed for the endogenous PU.1 gene.[15]

The zebrafish *(Danio rerio)* animal model offers a unique opportunity for the in vivo analysis of genes required for the control of normal vertebrate myeloid cell development. Embryonic zebrafish development is extremely rapid; rudiments of the major organs, including a functional heart and circulating blood cells, develop within 30 hours after fertilization. Zebrafish *pu.1 (zpu.1)* expression is detectable by whole-mount RNA in situ hybridization in hematopoietic cells between 12 and 30 hours after fertilization (hpf) but not in older embryos.[16,17] Expression of *zpu.1* is observed by 12 hpf in the anterior yolk region of the developing embryo, followed by expression in the posterior intermediate cell mass (ICM). The posterior expression is lost at approximately 24 hpf, whereas anterior expression persists and is observed in cells

From the Department of Pediatric Oncology, Dana-Farber Cancer Institute, Harvard Medical School, Boston, MA; Division of Hematology/Oncology, Beth Israel Deaconess Medical Center, Harvard Medical School, Boston, MA; Division of Hematology/Oncology, Children's Hospital Boston, Harvard Medical School, Boston, MA; Department of Pathology, Brigham and Women's Hospital, Boston, MA; and Division of Hematology, Brigham & Women's Hospital, Boston, MA.

Submitted September 10, 2003; accepted February 16, 2004. Prepublished online as Blood First Edition Paper, March 2, 2004; DOI 10.1182/blood-2003-09-3105.

Supported by grants CA93152 (A.T.L.) and CA96785 (K.H.), and the Dana-Farber/Harvard Cancer Center support grant CA006516, all from the National Institutes of Health, and the Leukemia and Lymphoma Society Specialized Center of Research (SCOR) Program.

The online version of the article contains a data supplement.

Reprints: A. Thomas Look, Department of Pediatric Oncology, Dana-Farber Cancer Institute, Boston, MA 02115; e-mail: thomas_look@dfci.harvard.edu.

The publication costs of this article were defrayed in part by page charge payment. Therefore, and solely to indicate this fact, this article is hereby marked "advertisement" in accordance with 18 U.S.C. section 1734.

spreading anteriorly over the yolk until 28 to 30 hpf. The *zpu.1*-expressing cells appear later in development than those expressing *scl, lmo2,* and *gata2,* which is consistent with findings in mammals, suggesting that the expression of *zpu.1* regulates the differentiation of hematopoietic stem cells along the myeloid lineage.

The use of a green fluorescent protein (GFP) transgene to study gene expression in zebrafish is particularly attractive since GFP fluorescence provides a rapid real-time approach for in vivo analysis of the spatial and temporal expression of developmentally regulated genes in the optically clear zebrafish embryo. Several GFP-expressing transgenic zebrafish lines have already been developed, allowing the study of gene expression and developmental processes (reviewed in Gong and Hew[18]). Although there are transgenic zebrafish models expressing GFP under the control of erythroid and lymphoid promoters, there is only one report of a transgenic zebrafish in which GFP is targeted to early myeloid cells of embryonic zebrafish.[19-21]

Here we report that a 9.0-kb fragment of zebrafish sequences upstream of the *zpu.1* initiator codon is able to drive GFP expression in myeloid cells from 12 to 28 hpf in a pattern overlapping the expression of endogenous *zpu.1* mRNA. Histologic sections from larval transgenic animals revealed GFP-expressing hematopoietic cells in the developing zebrafish kidney, which is the hematopoietic organ in adult teleosts. Analysis of cells from adult zebrafish kidney by flow cytometry and cell sorting revealed discrete subpopulations of GFP-positive cells, which exhibited either myeloid or lymphoid morphology, indicating that *zpu.1* is expressed in these cells during definitive hematopoiesis in adult zebrafish.

Materials and methods

Cloning and sequencing of zebrafish *zpu.1* genomic DNA

An arrayed zebrafish genomic bacterial artificial chromosome (BAC) library (Genome Systems, St Louis, MO) was screened with a ^{32}P-labeled zebrafish *pu.1* cDNA probe, resulting in the isolation of 2 positive clones, 184:L24 and 145:H24. The identities of the 2 isolated BAC clones were reconfirmed by polymerase chain reaction (PCR) using *zpu.1*-specific primers. BAC clone 184:L24 was used to generate the subsequent enhanced GFP-reporter plasmid constructs (Clontech, Palo Alto, CA).

Plasmid constructs

Construct 5pu.1-GFP was generated by ligating a 5-kb *PstI/NarI* fragment containing the putative zebrafish *pu.1* (*zpu.1*) promoter to a *GFP* reporter gene, enhanced *GFP (EGFP),* using a *NarI/Bam*HI linker containing the 5′ flanking sequences upstream of the putative *zpu.1* transcription start sites. The linker was amplified by the polymerase chain reaction (PCR) using a primer (Oligo 1, TTCCTACGGCCACTGTCAGG) complementary to genomic sequences just 5′ of the *NarI* site and a primer (Oligo 2, CGCGGATCCGCGGTTGGGTTCCTCGCCTCGCCTG) that is complementary to the cDNA sequence just 5′ of the *zpu.1* translation start. Primer (Oligo 2) contained a *Bam*HI site to facilitate subsequent cloning. PCR was carried out using the Advantage PCR System (Clontech) for 35 cycles (94°C, 30 seconds; 65°C, 30 seconds; 68°C, 2 minutes). After digestion with *Bam*HI and *Nhe*I, the amplified fragment was gel purified and ligated with the *PstI/NarI* fragment of the putative *zpu.1* promoter into the *Bam*HI-*Pst*I–digested *EGFP* vector (Clontech), resulting in construct 5pu.1-GFP. The construct 9zpu.1-GFP was generated by ligating an additional 4 kb of *zpu.1* genomic sequences upstream of the *Pst*I site to the 5′ end of the reporter gene in construct 5pu.1-GFP.

Microinjection of zebrafish embryos

The *PU.1*/GFP transgene was excised from plasmid vector of 9zpu.1-GFP by restriction digestion with *Afl* II and isolated following electrophoresis in low-melting agarose gel. DNA fragments were purified using Geneclean II Kit (Bio101 Inc, Montreal, QC, Canada) and resuspended in 5 mM Tris, 0.5 mM EDTA (ethylenediaminetetraacetic acid), and 0.1 M KCl at a final concentration of 100 mg/mL prior to microinjection. Single-cell wild-type embryos were injected as described.[22] Approximately 200 to 300 pg of linearized DNA were injected into one-cell–stage embryos.

Fluorescent microscopic observation and imaging

Embryos and adult fish were anesthetized using tricaine (Sigma A-5040; Sigma, St Louis, MO), as described previously,[23] and examined under a fluorescein isothiocyanate (FITC) filter on a fluorescent Leica microscope (MZFLIII) (Heidelberg, Germany) equipped with a Hammamatsu Orca 3CCD digital camera and accompanying software (Hammamatsu City, Japan).

Identification of germ line transgenic fish

Embryos injected with the 9zpu.1-GFP transgene were raised to maturity and incrossed. Embryos from these crosses were analyzed for GFP expression, isolated, and raised establishing a number of stable transgenic lines.

Whole-mount RNA in situ hybridization

Sense (control) and antisense digoxigenin (DIG)–labeled RNA probes were generated from a *zpu.1* cDNA clone (a gift from G. Lieschke, Ludwig Institute for Cancer Research, Melbourne, Australia). RNA in situ hybridizations were performed as described.[17] In double-labeling assays for detecting GFP and mRNA expression, embryos were processed for mRNA in situ hybridization as described[7]; however, prior to the antibody reaction for detecting the mRNA, the following steps were added for the visualization of GFP-positive cells. Anti-GFP–rabbit–conjugated antibody (Molecular Probes, Eugene, OR) was added at a final dilution of 1:1000 and embryos were incubated at 4°C overnight. The following morning, embryos were washed in blocking solution. Embryos were then incubated in 100 μL of 1:100 antirabbit Alexa (Molecular Probes) overnight at 4°C. Embryos were then washed 3 times for 20 minutes in blocking solution and incubated in anti-DIG–alkaline phosphatase–conjugated antibody at a final dilution of 1:5000 in blocking solution overnight at 4°C. The following morning, embryos were rinsed in blocking solution and then for 1 hour in Maleic acid buffer with Tween (MABT), followed by 30 minutes in MABT. After rinsing 3 times for 10 minutes each in Tris (pH 8.2) staining buffer, embryos were carefully transferred into 24-well cell culture plates for staining with Fast Red using tablets from Roche Biochemicals (Indianapolis, IN), according to the manufacturer's protocol. The staining reaction was performed in the dark to keep background staining to a minimum. Once the desired level of staining was seen, embryos were washed gently with copious amounts of phosphate-buffered saline with Tween (PBST). Embryos were then mounted in Vectashield Mounting Medium (Vector Laboratories, Burlingame, CA), and embryos were examined using a fluorescent microscope. RNA in situ hybridization on paraffin-embedded tissues was performed as described previously.[24] Confocal images were captured with a Zeiss LSM 510 META-NLO laser-scanning microscope and a Zeiss LD40× 0.6 NA Achroplan objective lens (Zeiss, Oberkochen, Germany).

Histology and cytology

Adult animals that were killed were placed in 4% paraformaldehyde at 4°C for 4 days and then transferred to 0.25 M EDTA (pH 8.0) for no fewer than 2 days. Fish were then dehydrated in alcohol, cleared in xylene, and infiltrated with paraffin. Four-micrometer tissue sections from paraffin-embedded tissue blocks were placed on charged slides, deparaffinized in xylene, rehydrated through graded alcohol solutions, and stained with hematoxylin/eosin. Cytospin preparations were performed using 1×10^5 to 2×10^5

kidney cells or splenocytes cytocentrifuged at 300 rpm for 3 minutes onto glass slides (Shandon, Waltham, MA). Blood smears and cytospin preparations were stained with May-Grünwald and Giemsa stains (Fluka, Buchs, Switzerland) for morphologic analyses and differential cell counts and were examined using an Olympus BX-51 microscope (Olympus, Melville, NY) equipped with a QImaging Micropublisher digital camera (QImaging, Burnaby, BC, Canada) and accompanying software.

Immunohistochemistry

Paraffin sections (4 μm) were used for immunohistochemical determination of GFP protein expression. Slides were deparaffinized and pretreated with 1.0 mM EDTA (pH 8.0; Zymed, South San Francisco, CA) in a steam pressure cooker (Decloaking Chamber; BioCare Medical, Walnut Creek, CA), according to the manufacturer's instructions, followed by washing in distilled water. All further steps were performed at room temperature in a hydrated chamber. Slides were pretreated with Peroxidase Block (DAKO, Carpinteria, CA) for 5 minutes to quench endogenous peroxidase activity, followed by goat serum diluted 1:5 in 50 mM Tris-Cl (pH 7.4) for 20 minutes at room temperature to block nonspecific binding sites. Primary murine antibody to GFP (Clone JL-8; Clontech) was applied at a 1:1000 dilution in 50 mM Tris-Cl (pH 7.4) with DAKO diluent (DAKO) for 1 hour. After washing in 50 mM Tris-Cl (pH 7.4), goat antibody to mouse horseradish peroxidase–conjugated antibody (Envision detection kit; DAKO) was applied for 30 minutes. Immunoperoxidase staining was developed with a diaminobenzidine (DAB) and chromogen kit (DAKO), according to the manufacturer's instructions, and examined using an Olympus BX41 microscope equipped with an Olympus QColor 3 camera and accompanying acquisition software.

Flow cytometry

Hematopoietic cells isolated from zebrafish were processed as described,[25] washed, and resuspended in ice-cold 0.9 × phosphate-buffered saline (PBS) + 5% fetal bovine serum (FBS) and passed through a 40-μm filter. Propidium iodide (PI; Sigma) was added to 1 μg/mL to exclude dead cells and debris. Fluorescence-activated cell sorter (FACS) analysis and sorting was performed based on PI exclusion, forward scatter, side scatter, and GFP fluorescence using a FACS Vantage flow cytometer (Becton Dickinson, Franklin Lakes, NJ). Target cell populations were sorted twice to optimize cell purity. Mean cell sizes of scatter populations were determined by linear normalization to 2-μm and 10-μm latex beads using forward scatter.[25]

RT-PCR analysis

GFP-positive, FACS-sorted blood cell populations were obtained from adult zebrafish kidneys and transferred into an RNase-free tube containing 100 μL of Trizol (Gibco, Carlsbad, CA) and 25 μg of glycogen (Ambion, Austin, TX). Total RNA was extracted from 1000 to 2000 sorted cells, according to the manufacturer's protocol, and then resuspended into 10 to 20 μL of diethyl pyrocarbonate (DEPC) water. Total RNA aliquots corresponding to 10 or 100 cells were used as template, and One-step reverse transcriptase–PCR (RT-PCR; Qiagen, Valencia, CA) was performed in a volume of 25 μL. Ten-nanogram aliquots of total kidney cell RNA and 100 cells aliquots from the GFP-negative "lymphoid compartment" were used as controls. All primers except *ZlgLC3* and *Zrag2* primers were designed to span one or more introns. Primer sequences for zebrafish genes in the lymphoid lineages[26] are as follows: *rag2* (forward, ACGCTCATGTCCAACTGGGATAT; and reverse, TTGAGGCGGACAGTCACCTACACT); *IgLC3* (forward, GTTCCTGACCAGTGCAGAGA; and reverse, CCTGATCACCTCCAGCATGA); and *lck* (forward, AGATGAATGGTGTGACCAGTGTA; and reverse, GATCCTGTAGTGCTTGATGATGT). Primer sequences of the other zebrafish genes are as follows: *mpo* (forward, GCTGCTGTTGTGCTCTTTCA; and reverse, TTGAGTGAGCAGGTTTGTGG); *gata1* (forward, ATTATTCCACCAGCGTCCAG; and reverse, CCACTTCCACTCATGGGACT); *pu.*1 (forward, CAGAGCTACAAAGCGTGCAG; and reverse, GCAGAAGGTCAAGCAGGAAC); α-*hemaglobin* (forward, TTGTCTACCCCCAGACCAAG; and reverse, AGAGCCAGAGCTGAGAGGAA); scl (forward, AGCCATAAGGTGCAGACCAC; and reverse, CGTTGAGGAGCTTAGCCAGA); and β-*actin* (forward, CCCAGACATCAGGGAGTGAT; and reverse, CACCGATCCAGACGGAGTAT). RT-PCR conditions are as follows: 50°C, 32 minutes; 95°C, 15 minutes; 35 cycles of 94°C, 30 seconds; 60°C, 30 seconds; 72°C, 1 minute; then 72°C, 10 minutes; 4°C stored. PCR products were separated on a 1.2% agarose gel.

Results

The zpu.1 promoter directs EGFP expression in transgenic zebrafish

To study the development of early myeloid subpopulations, we tested the ability of promoter fragments of *zpu.1* to drive EGFP expression in the myeloid cells of transgenic lines.[16,17] An *Eco*RI and *Nar*I restriction fragment was found to span approximately 9 kb of sequences upstream of the *zpu.1* initiation codon (Figure 1A). A linker spanning the *Nar*I site and the 5′ untranslated region (UTR) just upstream of the *zpu.1* start codon was amplified by PCR and used to insert the 9-kb *Eco*RI-*Nar*I fragment upstream of EGFP into pSKII (Figure 1B). Injection of this construct (referred to as 9zpu.1-EGFP) into one-cell–stage zebrafish embryos resulted in EGFP expression within myeloid cells migrating over the anterior yolk at 22 hpf (Figure 1C white arrowhead). Expression in muscle cells of the trunk was also noted (Figure 1C yellow arrowhead). To establish stable transgenic lines, one-cell–stage embryos injected with linearized 9zpu.1-EGFP were grown to adulthood. Ninety adults were grown from injected embryos and 7 transgenic founders were identified as capable of producing offspring that expressed the EGFP transgene within 24 hpf (Table 1). The transmission rates varied from 4% to 50% among the progeny of the transgenic founders, indicating germ cell mosaicism in genomic transgene integration,

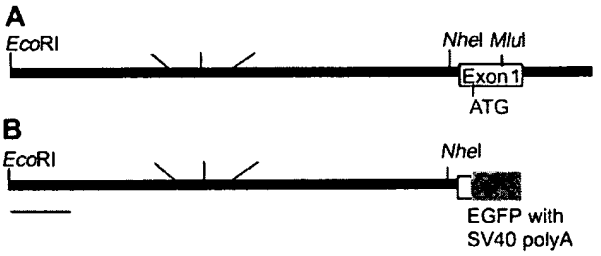

Figure 1. Structure of the *zpu.1* promoter and transient expression of EGFP. (A) Restriction map of the genomic region upstream of the first exon of *zpu.1*. (B) Restriction map of the *zpu.1* genomic fragment and the EGFP transgene in the 9pu.1-EGFP construct used for injection to establish transgenic lines. (C) Fluorescent image of 22 hpf living embryos injected with linearized 9pu.1-GFP at the one-cell stage. The white arrowhead indicates zpu.1-expressing myeloid cells migrating from the anterolateral mesoderm over the yolk; and the yellow arrowhead, fluorescence in skeletal muscle. Lateral views, anterior is to the left, dorsal is up. Original magnification × 40.

Table 1. Comparison of expression levels in transgenic founders

Allele	Hematopoietic expression level	Nonhematopoietic expression level
1	++	Muscle
2	++	Muscle, eye
3	+	Muscle
4	+	Muscle
5	+++	Muscle, CNS
6	–	Global
7	–	Global

The official name for these lines is *TG(zpu.1:EGFP)*. Expression level was determined by observation at 24 hpf using a dissection microscope equipped with epifluorescence.

+, ++, and +++ indicate relative expression levels; CNS, central nervous system; and –, not observed.

consistent with previous transgenic fish reports.[18,27] All of the transgenic founders produced embryos that expressed EGFP at detectable levels using a dissecting microscope equipped with epifluorescence. However, individual founder lines displayed different levels of EGFP expression and some lines exhibited either ectopic expression in the brain and eyes or ubiquitous expression (Table 1). The lines were assigned names according to standard zebrafish nomenclature and are hereafter referred to as *TG(zpu.1:EGFP)* with allele designations *df1* through *df7*. The rate of transgene transmission in the F2 incross of F1 brothers and sisters, each of whom harbored the transgene, was consistent with a dominant mendelian inheritance ratio (approximately 75%), suggesting that each transgene was integrated into a single chromosome locus. So far, the stable transmission and expression of the EGFP transgene have been maintained over 3 generations. For all studies described in this report, allele *5* (*TG(zpu.1:EGFP)^{df5}*) was used because it exhibited the brightest EGFP fluorescence in developing myeloid cells.

EGFP expression pattern in transgenic embryos

EGFP expression in the *TG(zpu.1:EGFP)^{df5}* line was detected at low levels as early as the 6-somite stage within the anterior-lateral mesoderm when the endogenous *zpu.1* transcript is first detectable by in situ hybridization.[16] By 22 hpf, the pattern of expression EGFP in the transgenic line was also indistinguishable from that of endogenous *zpu.1* RNA and was observed in the anterior-lateral mesoderm and in the posterior ICM, with EGFP-expressing cells spreading over the yolk cell (Figure 2A-C). Confocal coexpression studies using an anti-GFP antibody and an antisense zebrafish *zpu.1* mRNA probe revealed that 95% of cells expressed both GFP and pu.1 mRNA (Figure 2D yellow cells). At 24 hpf, the ectopic EGFP expression in muscle and hindbrain became evident and persisted through early larval stages (data not shown). Endogenous *zpu.1* mRNA is not detectable in these locations, suggesting that this aspect of the EGFP expression in these lines is ectopic and may result from the lack of regulatory sequences in the 9 kb of *zpu.1* promoter that are responsible for suppressing embryonic muscle and neural *zpu.1* expression.

EGFP expression in transgenic zebrafish larvae

In the zebrafish, embryonic *zpu.1* expression is undetectable by RNA in situ hybridization after 30 hpf.[16,17] After 7 to 10 days after fertilization (dpf) and throughout adulthood, the major site of definitive hematopoiesis in the zebrafish is within the interstitium of the kidney, known as the "kidney marrow."[28] In the free-swimming larvae of fish and amphibians, the pronephros, consisting of bilateral tubules and glomeruli, forms first and later gives rise to the mesonephros, which contains the renal tubules (reviewed in Drummond[29]). Immunohistochemical examination of tissue sections from 20-day-old *TG(zpu.1:EGFP)^{df5}* transgenic larvae provided evidence of EGFP expression by cells in kidney and other tissues (Figure 3A), which was not detectable by epifluorescence analysis of living fish. We found evidence of GFP-positive hematopoietic cells in the interstitial kidney marrow cells located between the glomeruli in the pronephros (Figure 3B-C) in a region also known to contain *gata1*-positive cells.[20] By contrast, EGFP-expressing cells were not evident in the mesonephros at this stage of development. We also detected EGFP expression in the muscle cells of the larvae (Figure 3D), consistent with our observations in living embryos.

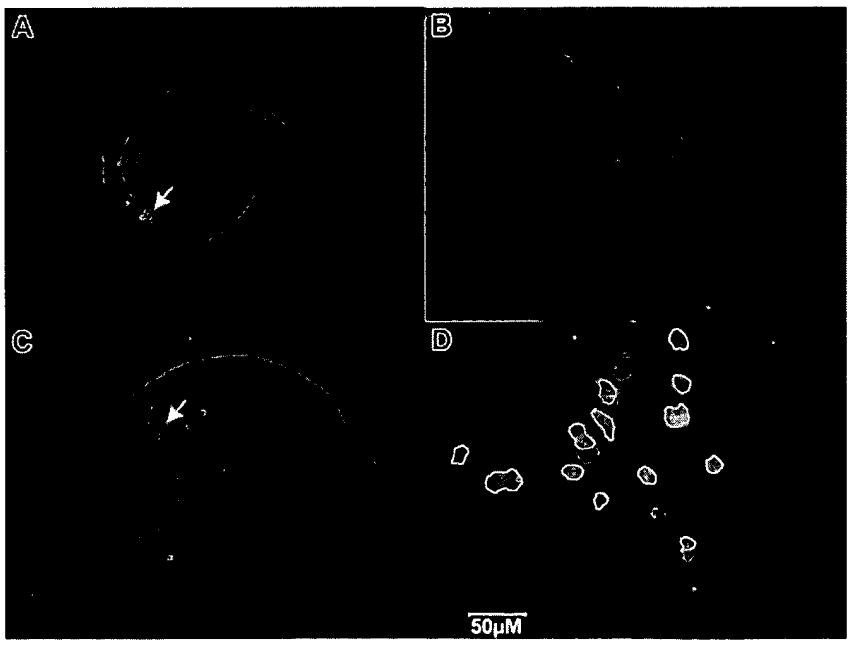

Figure 2. Fluorescent images of *TG(zpu.1:EGFP)^{df5}* embryos at 22 hpf. (A) Lateral view of GFP-positive cells. (B) Magnified lateral view of the posterior tail in panel A. (C) Dorsal view of the anterior head region. The white arrows indicate *zpu.1*-expressing myeloid cells migrating from the anterolateral mesoderm over the yolk; and the red arrows, *zpu.1* cells in the ICM. (D) Confocal image of 2-color in situ hybridization of cells migrating over the anterior yolk at 22 hpf using a *zpu.1* RNA probe (red) and an antibody to EGFP (green). Yellow indicates coexpression. Original magnification × 40 (A, D); × 100 (B-C).

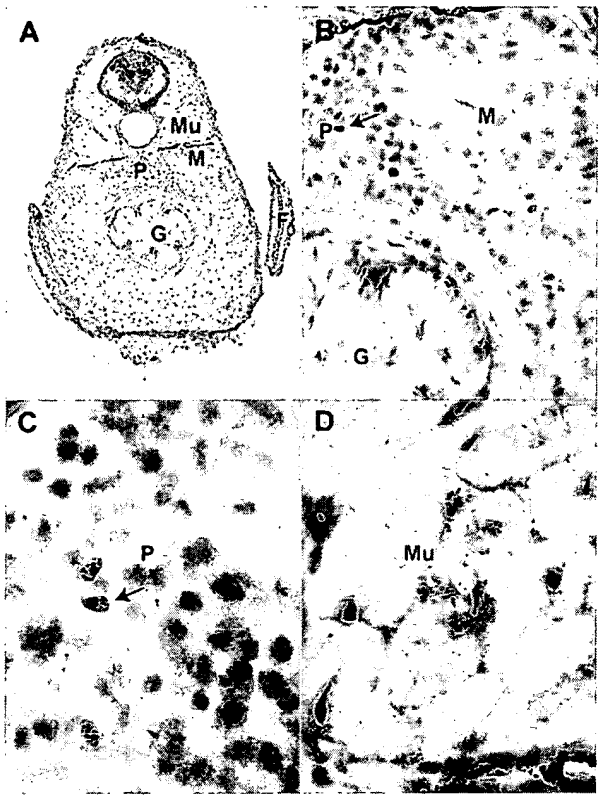

Figure 3. Immunohistochemistry of *TG(zpu.1:EGFP)*^{dt5} 20-day-old transgenic larvae. (A) Transverse section at the level of the pectoral fin (F) showing the pronephros (P), mesenephros (M), muscle (Mu), and gut (G). Enlarged views of the (B) mesonephros and pronephros junction, (C) pronephros, and (D) muscle. Original magnifications × 100 (A), × 200 (B), and × 1000 (C-D). Arrows indicate positive cells.

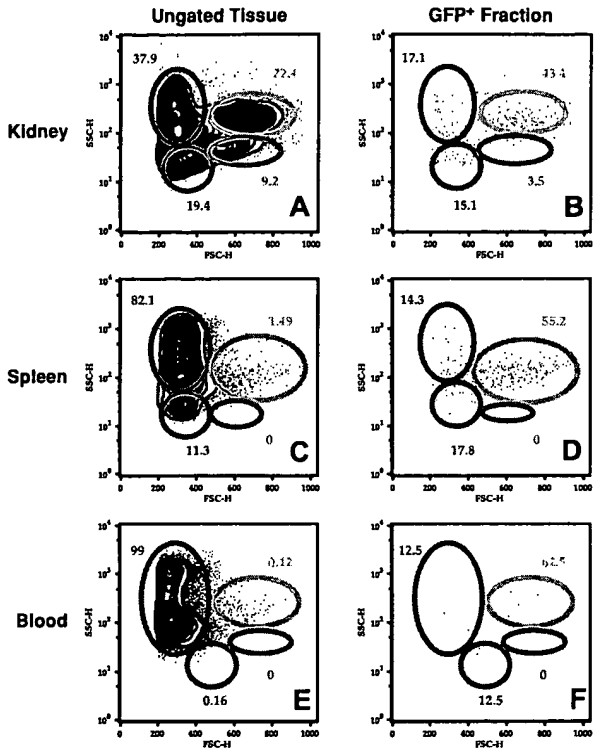

Figure 5. FACS analysis of hematopoietic cells from the *TG(zpu.1:EGFP)*^{dt5} adult fish. Cells from kidney (A-B), spleen (C-D), and blood (E-F) from adult transgenic zebrafish were isolated and analyzed by FACS for total cellular subfractions by light-scatter gating (A,C,E) and the same subfractions of EGFP-positive cells (B,D,F). Gated populations are as follows: erythrocytes (red), lymphocytes (blue), granulocytes and monocytes (green), and blood cell precursors (purple). Cell size is represented by forward scatter (FSC; abscissa), and granularity is represented by side scatter (SSC; ordinate). Mean percentage of cells is indicated for each gated subpopulation.

EGFP expression in adult transgenic zebrafish kidney

We examined tissue sections of adult zebrafish (6 months old) for EGFP expression by immunohistochemistry (Figure 4A). In adults, EGFP expression was no longer detectable in muscle cells and was restricted to a small fraction of cells in the kidney marrow. At this stage, development of the zebrafish kidney is complete, and hematopoietic cells are situated between the renal tubules (Figure 4B). A small number of hematopoietic cells were found to be EGFP-positive (Figure 4C), similar to the number of *pu.1*-positive cells observed by RNA in situ hybridization on similar sections from the same fish (Figure 4D).

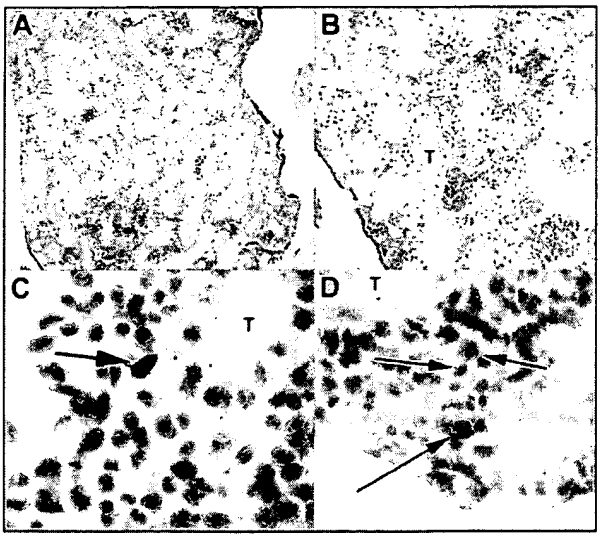

Figure 4. Immunohistochemistry of *TG(zpu.1:EGFP)*^{dt5} adult kidney marrow. (A-C) Transverse sections showing EGFP-positive cells in the kidney marrow of transgenic adults at progressively increased magnification, and (D) transverse section of the kidney of transgenic fish analyzed with zebrafish *pu.1* antisense RNA. T indicates renal tubule. Original magnifications × 100 (A), × 200 (B), and × 1000 (C-D). Arrows indicate positive cells.

To identify the hematopoietic cells expressing EGFP driven by the zpu.1 promoter, we examined living cells from the kidney, spleen, and blood by FACS. In our transgenic fish, the cells expressing EGFP accounted for 1.8% ± 0.3% (n = 8) of all hematopoietic cells in the kidney, and they were enriched in the myeloid and "lymphoid" cell light-scatter gates (Figure 5A-B). In the spleen, EGFP-expressing cells accounted for 1.1% ± 0.4% (n = 6) of the cells, with the majority of these cells falling within the myeloid scatter fraction (Figure 5C-D). In the blood, only a very small fraction (0.0086%) of cells expressed EGFP, predominantly within the myeloid cell population (Figure 5E-F). We used cell sorting to analyze the morphology of the EGFP-positive kidney marrow cells in the lymphoid (Figure 6A) and myeloid (Figure 6B) compartments. By analysis of May-Grünwald–stained cells, the cells in the lymphoid compartment had the appearance lymphoid or undifferentiated early progenitor cells (Figure 6C), while cells in the myeloid compartment were predominantly monocytic or bilobed neutrophilic precursors, suggesting that *zpu.1* is down-regulated at the metamyelocyte stage, relatively late in myeloid cell development (Figure 6D). Likewise, cells in the

myeloid compartment expressed both *zpu.1* and *zmpo*, as demonstrated by RT-PCR at the 10-cell level (Figure 7 top, lanes 4-5) and 100-cell level (data not shown). The fact that GFP-positive cells in the lymphoid compartment expressed *zpu.1* (Figure 7 bottom, lane 4) but lacked the expression of zebrafish *mpo* or the lymphoid markers *lck*, *rag2*, and *Ig light chain*[26] at the 10-cell level (Figure 7 bottom, lanes 1-3) and 100-cell level (data not shown), suggests that these cells represent early hematopoietic or immature lymphoid cells. To further analyze the GFP-positive cells in the lymphoid compartment, we also examined expression of the stem cell marker *scl*. The cells also did not express *scl* at the 10- and 100-cell levels (Figure S1; see the Supplemental Figure link at the top of the online article on the *Blood* website). Thus the GFP-positive cells in our study with light-scatter properties similar to lymphoid cells lack expression of any of the markers of differentiated hematopoietic cells that were tested except *zpu.1*, suggesting that they represent early hematopoietic cells that lack *scl* expression or immature lymphoid cells.

Discussion

Vertebrate hematopoiesis is a complex process that proceeds in distinct phases at changing anatomical sites during development.[30] Developmentally regulated transcription factors, including PU.1, play essential roles in controlling this process. In this study, we used the zebrafish animal model and generated transgenic lines using the *zpu.1* promoter to drive the expression of EGFP in developing myeloid cells during embryogenesis and in the adult. Our results during embryonic development are similar to those reported by Ward et al,[21] indicating that either 5.3- or 9.0-kb genomic fragments are able to drive EGFP expression in *zpu.1*-expressing cells during zebrafish embryogenesis. However, the recently published papers of Ward et al[21] and others[16,17] examined *zpu.1* expression only during zebrafish embryogenesis and did not address the lineage-restricted expression pattern of this transcription factor during definitive hematopoiesis in juvenile and adult zebrafish.

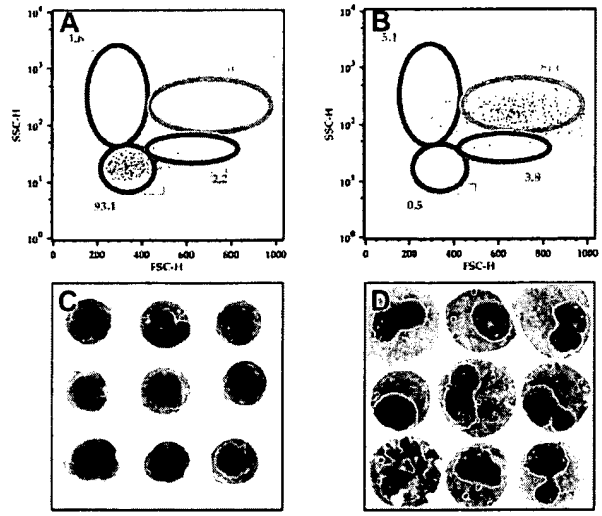

Figure 6. FACS analysis and morphology of hematopoietic cells from the *TG(zpu.1:EGFP)*^{dt5} adult kidney. GFP-sorted cells were further separated into lymphoid (A) and myeloid (B) compartments, and morphology for the lymphoid-sorted (C) and myeloid-sorted (D) cells was evaluated by cytospin. Gated populations are as described.[25] Populations of cells within each gate are described as mean percentages of total cells. Original magnification × 1000 (C-D).

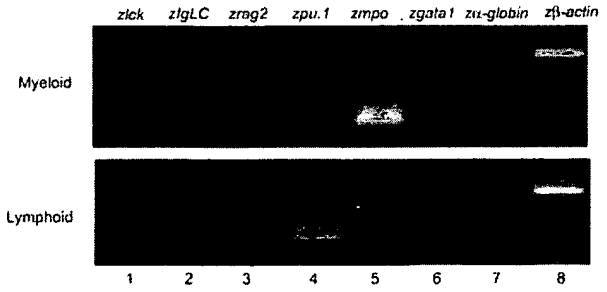

Figure 7. RT PCR analysis of hematopoietic cells from the *TG(zpu.1:EGFP)*^{dt5} adult kidney. GFP-sorted cells from the myeloid and lymphoid light-scatter compartments were analyzed for lineage-specific expression of the zebrafish *lck*, *lgLC*, *rag2*, *pu.1*, *mpo*, *gata1*, *α-hemaglobin*, and *β-actin* genes.

By examining the developing zebrafish kidney at 20 dpf, we were able to identify EGFP-positive cells in the region of the developing pronephros, the site of definitive hematopoiesis in juvenile fish. EGFP-expressing cells were also present in low numbers in the adult kidney marrow. Further analysis by FACS revealed that these EGFP-positive cells are predominantly myeloid or lymphoid/early hematopoietic cells, indicating that the *pu.1* promoter fragment described here is useful for identifying the myeloid and immature hematopoietic cell populations that express this gene and that, as in mammals, *zpu.1* is expressed during definitive myelopoiesis. The ectopic EGFP expression in the muscle of transgenic embryos may be due to the lack of a transcriptional silencer in our 9.0-kb promoter fragment that normally suppresses nonhematopoietic cell expression of *pu.1*. The aberrant EGFP expression in muscle cells, which was observed in all 7 stable transgenic lines, appears to be restricted to embryogenesis, since EGFP expression was not detected in muscle cells of adult zebrafish.

Our studies indicate that in older zebrafish, *zpu.1* is expressed in cells with the morphology of immature lymphoid/hematopoietic cells or myeloid cells (Figure 6). Lineage-specific gene expression analysis suggests that *zpu.1* is expressed during myeloid differentiation in adults with eventual coexpression of both *zpu.1* and *zmpo*, as has been observed during embryonic development.[17] In contrast, *zpu.1* is expressed by lymphoid appearing cells that do not express *zlck*, *zRag2*, *zlgLC*, and *zmpo*, suggesting that *zpu.1* is expressed by more primitive progenitor cells that lack expression of the marker genes of hematopoietic differentiation that were studied here. Previous embryonic studies did not show evidence of *zpu.1* expression by whole-mount RNA in situ hybridization after 30 hpf[16,17]; however, *zpu.1* expression was detectable by RT-PCR in embryos as old as 7 dpf.[16] The detection of EGFP expression in juvenile and adult fish in a small subset of hematopoietic cells supports the hypothesis that *zpu.1* is expressed by subsets of myeloid progenitor and other immature hematopoietic cells throughout zebrafish development.

Zebrafish have a number of features that facilitate the study of vertebrate hematopoiesis. Because fertilization of eggs is external and embryos are nearly transparent, the cell movement and behavior of labeled hematopoietic cells can be directly monitored in vivo. In addition, many mutants that are defective in hematopoietic development have been generated.[31,32] Zebrafish embryos that lack circulating blood cells can survive for several days, so downstream effects of mutations can be analyzed even if specific genes are inactivated in ways that are deleterious to embryonic development. Since the genes and molecular regulation of hematopoiesis are highly conserved throughout vertebrate evolution, results from zebrafish embryonic studies can provide insight into the mechanisms involved in mammalian hematopoiesis.

The stable transgenic zebrafish lines expressing EGFP in subsets of hematopoietic cells have many important uses for future studies of mechanisms regulating hematopoiesis. By capitalizing on the capacity

of the zebrafish model to accommodate forward-genetic mutagenesis screens, the *TG(zpu.1:EGFP)*^{nl5} line will be useful to help identify genes that influence myeloid and lymphoid/progenitor cell development. Adoptive transfer experiments using these EGFP-expressing cells will establish their lineage reconstituting capacity. Furthermore, transgenic zebrafish lines are valuable for the study of molecular pathways in leukemogenesis.[24] Thus, the 9.0-kb *zpu.1* promoter fragment described here, which is able to drive *zpu.1* expression in the myeloid cells of adult zebrafish, should provide a useful means to drive the expression of oncogenes during myelopoiesis to facilitate the development of zebrafish models of acute myeloid leukemia.

Acknowledgments

We thank Min Deng, Hui-Ying Piao, Alan Flint, Janice Williams, Yu Yang, David Langenau, and Vuong Nguyen for their technical help and support.

References

1. Klemsz MJ, McKercher SR, Celada A, Van Beveren C, Maki RA. The macrophage and B cell-specific transcription factor PU.1 is related to the ets oncogene. Cell. 1990;61:113-124.
2. Hromas R, Orazi A, Neiman RS, et al. Hematopoietic lineage- and stage-restricted expression of the ETS oncogene family member PU.1. Blood. 1993;82:2998-3004.
3. Galson DL, Hensold JO, Bishop TR, et al. Mouse beta-globin DNA-binding protein B1 is identical to a proto-oncogene, the transcription factor Spi-1/PU.1, and is restricted in expression to hematopoietic cells and the testis. Mol Cell Biol. 1993;13:2929-2941.
4. Chen HM, Zhang P, Voso MT, et al. Neutrophils and monocytes express high levels of PU.1 (Spi-1) but not Spi-B. Blood. 1995;85:2918-2928.
5. Tenen DG, Hromas R, Licht JD, Zhang DE. Transcription factors, normal myeloid development, and leukemia. Blood. 1997;90:489-519.
6. Voso MT, Burn TC, Wulf G, Lim B, Leone G, Tenen DG. Inhibition of hematopoiesis by competitive binding of transcription factor PU.1. Proc Natl Acad Sci U S A. 1994;91:7932-7936.
7. Scott EW, Simon MC, Anastasi J, Singh H. Requirement of transcription factor PU.1 in the development of multiple hematopoietic lineages. Science. 1994;265:1573-1577.
8. McKercher SR, Torbett BE, Anderson KL, et al. Targeted disruption of the PU.1 gene results in multiple hematopoietic abnormalities. EMBO J. 1996;15:5647-5658.
9. Rekhtman N, Radparvar F, Evans T, Skoultchi AI. Direct interaction of hematopoietic transcription factors PU.1 and GATA-1: functional antagonism in erythroid cells. Genes Dev. 1999;13:1398-1411.
10. Zhang P, Zhang X, Iwama A, et al. PU.1 inhibits GATA-1 function and erythroid differentiation by blocking GATA-1 DNA binding. Blood. 2000;96:2641-2648.
11. Wang X, Scott E, Sawyers CL, Friedman AD. C/EBPalpha bypasses granulocyte colony-stimulating factor signals to rapidly induce PU.1 gene expression, stimulate granulocytic differentiation, and limit proliferation in 32D cl3 myeloblasts. Blood. 1999;94:560-571.
12. Moreau-Gachelin F, Wendling F, Molina T, et al. Spi-1/PU.1 transgenic mice develop multistep erythroleukemias. Mol Cell Biol. 1996;16:2453-2463.
13. Chen H, Ray-Gallet D, Zhang P, et al. PU.1 (Spi-1) autoregulates its expression in myeloid cells. Oncogene. 1995;11:1549-1560.
14. Chen H, Zhang P, Radomska HS, Hetherington CJ, Zhang DE, Tenen DG. Octamer binding factors and their coactivator can activate the murine PU.1 (spi-1) promoter. J Biol Chem. 1996;271:15743-15752.
15. Li Y, Okuno Y, Zhang P, et al. Regulation of the PU.1 gene by distal elements. Blood. 2001;98:2958-2965.
16. Lieschke GJ, Oates AC, Paw BH, et al. Zebrafish SPI-1 (PU.1) marks a site of myeloid development independent of primitive erythropoiesis: implications for axial patterning. Dev Biol. 2002;246:274-295.
17. Bennett CM, Kanki JP, Rhodes J, et al. Myelopoiesis in the zebrafish, Danio rerio. Blood. 2001;98:643-651.
18. Gong Z, Hew CL. Transgenic fish in aquaculture and developmental biology. Curr Top Dev Biol. 1995;30:177-214.
19. Jessen JR, Willett CE, Lin S. Artificial chromosome transgenesis reveals long-distance negative regulation of rag1 in zebrafish. Nat Genet. 1999;23:15-16.
20. Long Q, Meng A, Wang H, Jessen JR, Farrell MJ, Lin S. GATA-1 expression pattern can be recapitulated in living transgenic zebrafish using GFP reporter gene. Development. 1997;124:4105-4111.
21. Ward AC, McPhee DO, Condron MM, et al. The zebrafish spi1 promoter drives myeloid-specific expression in stable transgenic fish. Blood. 2003;102:3238-3240.
22. Culp P, Nusslein-Volhard C, Hopkins N. High-frequency germ-line transmission of plasmid DNA sequences injected into fertilized zebrafish eggs. Proc Natl Acad Sci U S A. 1991;88:7953-7957.
23. Westerfield M. The Zebrafish Book. Eugene, OR: University of Oregon Press; 1995.
24. Langenau DM, Traver D, Ferrando AA, et al. Myc-induced T cell leukemia in transgenic zebrafish. Science. 2003;299:887-890.
25. Traver D, Paw BH, Poss KD, Penberthy WT, Lin S, Zon LI. Transplantation and in vivo imaging of multilineage engraftment in zebrafish bloodless mutants. Nat Immunol. 2003;4:1238-1246.
26. Langenau DM, Ferrando AA, Traver D, et al. In vivo tracking of T cell development, ablation, and engraftment in transgenic zebrafish. Proc Natl Acad Sci U S A. 2004;101:7369-7374.
27. Stuart GW, McMurray JV, Westerfield M. Replication, integration and stable germ-line transmission of foreign sequences injected into early zebrafish embryos. Development. 1988;103:403-412.
28. Zapata A. Ultrastructural study of the teleost fish kidney. Dev Comp Immunol. 1979;3:55-65.
29. Drummond I. Making a zebrafish kidney: a tale of two tubes. Trends Cell Biol. 2003;13:357-365.
30. Zon LI. Developmental biology of hematopoiesis. Blood. 1995;86:2876-2891.
31. Weinstein BM, Schier AF, Abdelilah S, et al. Hematopoietic mutations in the zebrafish. Development. 1996;123:303-309.
32. Ransom DG, Haffter P, Odenthal J, et al. Characterization of zebrafish mutants with defects in embryonic hematopoiesis. Development. 1996;123:311-319.

APPENDIX F

1: J Leukoc Biol. 2006 Dec;80(6):1281-8. Epub 2006 Sep 8.

Resolution of inflammation by retrograde chemotaxis of neutrophils in transgenic zebrafish.

Mathias JR, **Perrin BJ**, **Liu TX**, **Kanki J**, **Look AT**, **Huttenlocher A**.

University of Wisconsin-Madison, 2715 Medical Sciences Center, 1300 University Ave., Madison, WI 53706, USA.

Neutrophil chemotaxis to sites of inflammation is a critical process during normal immune responses to tissue injury and infection and pathological immune responses leading to chronic inflammation. Although progress has been made in understanding the mechanisms that promote neutrophil recruitment to inflamed tissue, the mechanisms that regulate the resolution phase of the inflammatory response have remained relatively elusive. To define the mechanisms that regulate neutrophil-mediated inflammation in vivo, we have developed a novel transgenic zebrafish in which the neutrophils express GFP under control of the myeloperoxidase promoter (zMPO:GFP). Tissue injury induces a robust, inflammatory response, which is characterized by the rapid chemotaxis of neutrophils to the wound site. In vivo time-lapse imaging shows that neutrophils subsequently display directed retrograde chemotaxis back toward the vasculature. These findings implicate retrograde chemotaxis as a novel mechanism that regulates the resolution phase of the inflammatory response. The zMPO:GFP zebrafish provides unique insight into the mechanisms of neutrophil-mediated inflammation and thereby offers opportunities to identify new regulators of the inflammatory response in vivo.

PMID: 16963624 [PubMed - indexed for MEDLINE]